Investigation of the spectroscopic, chemical and physical properties of Cyrene and its hydrate

Antonio Misefari

MSc by Research

University of York

Chemistry

April 2017

Abstract

This work examines distinct properties of Cyrene notably the occurrence of a carbonyl doublet in the IR spectrum and the formation of the Cyrene-hydrate (= Cyrene's geminal diol) when mixing Cyrene with water. To this extent a thorough analysis by FT-IR, Raman, ^{1}H NMR and ^{13}C NMR spectroscopy was undertaken. FT-IR spectroscopy was also performed with variable temperatures as to gain more understanding on the chemical/physical reasons for the carbonyl doublet presence. Surprisingly limited influence of this phenomenon by both temperature and use of different solvents was seen. The possible occurrence of Fermi resonance was also investigated but Raman spectroscopy, using polarized and non-polarized light, largely ruled out this hypothesis. Calculation of the IR spectrum of pure Cyrene was also performed suggesting the occurrence of Cyrene dimers in the least – potentially extending into oligomeric structures. The presence of such structures are consistent with the high value of the enthalpy of vaporization as calculated by the classic Clausius Clapeyron equation. Calorimetric analysis (covering the -70 to 20 °C range) of both pure Cyrene and its solutions in different solvents was equally performed. The data suggested an amorphous structure, not showing a unique and consistent peak for the crystallization and melting point. Also, a strong dependence of the thermograph on the thermal history of the sample could be observed. Analysis by diffuse light scattering (DLS), small angle X-ray scattering (SAXS) and polarized light microscopy ruled out the occurrence of a long-range structural order (as one can encounter with ionic liquids and liquid crystals) for Cyrene. The Cyrene hydrate case was found very complex in that mixing Cyrene with water yielded a ternary mixture consisting of Cyrene, its hydrate or geminal diol and remaining unreacted water. This was established by state of the art solvent free ^{1}H and ^{13}C NMR analysis. Density and viscosity measurements of Cyrene/water combinations revealed two distinct zones: a) the addition of >50 wt% Cyrene to water is characterized by high densities and viscosities b) <50 wt% Cyrene in water the properties are largely dominated by the water component. NMR at different temperatures was also performed showing that an increase in the temperature shifts the Cyrene/geminal diol equilibrium to Cyrene and a decrease in the temperature favours the Cyrene hydrate. Interestingly the Cyrene/geminal diol equilbrium does not fit the intuitive stoichiometry of one water molecule reacting with one Cyrene to form a single geminal diol. It is shown that at least two waters are implicated in this equilibrium, hinting at the formation of clathrates. Interestingly the presence of Cyrene and geminal diol in water actively depresses the latter's freezing point much alike in water/ethylene glycol mixtures. Also, the ternary mixture is a clear example of a NAtural Deep Eutetic Solvent (NADES) but then, unusually, as a solvent mixture. Lastly the solubility of a range of compounds was investigated in a range of Cyrene/geminal diol/water ternary mixtures. To this end solvent-free ^{1}H and ^{13}C NMR spectroscopy was used. Through this investigation it was found that the ternary mixture can be exploited as a chameleon solvent and a switchable hydrotrope. On the one side, the addition of a small amount of water to Cyrene switches on the amphiphilic geminal diol chameleon solvent, increasing the solubility of a range of compounds vis-à-vis their solubility in pure Cyrene with up to a factor of 9. Alternatively, the addition of Cyrene to water creates in situ the amphiphilic geminal diol as a switchable hydrotrope, which leads to a remarkable increase in solubility up to 10000-fold. The dissolved compounds can generally be recovered by simply adding (or removing) water, potentially aided by lowering the temperature, decreasing naturally their solubility.

Table of content

List of the tables

List of figures

List of abbreviations

Cyrene	Dihydrolevoglucosenone
NMR	Nuclear Magnetic Resonance
FT-IR	Fourier transform-Infrared spectroscopy
DLS	Dynamic light scattering
SAXS	Small angle X-ray scattering
NADES	NAtural Deep Eutetic Solvent
ESR	Electron spin resonance spectroscopy
HBD	Hydrogen bond donor ability
δ	Delta
α	Alpha
E_T^N	Normalised polarity
DMAC	N,N-dimethylacetamide
DMF	N,N-dimethylformamide
NMP	N-methylpyrrolidone
Keq	Equilibrium constant
wt%	Weight percentage

Acknowledgements

Firstly, I would like to thank Professor James Clark for having given me the opportunity to work in his laboratory on a range of very interesting topics in the broad area of Cyrene. Special thanks go also to Dr. Mario De bruyn who spent many hours co-developing the experiments and discussing the obtained results over numerous coffees in the Kitchen. Additionally his efforts to get me a better English level – also assisted by his lovely wife Catherine De bruyn – are much much appreciated. I am also indebted to Dr. Andrew Hunt for the tireless corrections of my thesis and the many constructive comments. Specifically to the infrared experiments I would like to thank Mr. Paul Elliott and Dr. Vitaliy Budarin for the technical and practical help. Dr. Martin Cockett is greatly acknowledged for his efforts in calculating/modelling the IR spectra of liquid Cyrene. I also would like to thank Dr. Lucia D'Andrea for her help with the SAXS experiments and in extension also Dr. John Slatter for discussions on the obtained results and his willingness to let me use some of the instruments in his laboratory. I also would like to acknowledge here Dr. Seishi Shimizu, Dr. James Sherwood and Mr. Tom Nicol for their help on the thermodynamic aspects of this thesis. A thank you also to Ms. Charlotte Brannigan for her help with Karl Fischer titration. Thank you also to Dr. Andrew Leech for the training on the density meter and Dr. Konstantinos Chatzipanagis for the help provided with the Raman measurements.

Special thanks also to my girlfriend Raquel for the non-scientific part to this thesis and the wonderful moments in York. And finally a massive thank you to my family for their continued moral and financial support without which I would not have been able to do this master.

Declaration

I declare that this thesis is a presentation of original work and I am the sole author. This work has not previously been presented for an award at this, or any other, University. All sources are acknowledged as References. The NMR spectra on Cyrene's geminal diol were obtained from Dr. Mario De bruyn. The author of this manuscript participated though intensely in the discussion of these, and related results, adding substantially to the draft article written on this particular topic (mainly chapter 3 - currently under review by Green Chemistry). Dr. Martin Cockett has performed the theoretical calculations of the IR spectra of liquid Cyrene. The Raman spectra were practically recorded by Dr. Konstantinos Chatzipanagis – *a postdoctoral fellow linked to the Department of Physics at the University of York*. Dr. Lucia d'Andrea performed the SAXS experiments. All other results are the work of the author.

Chapter 1: *Introduction and literature review*

Chapter 1

1 INTRODUCTION

1.1 Aims of the work

In this work a range of unusual properties of Cyrene are being investigated centered particularly on the occurrence of a carbonyl doublet in the IR spectrum and the formation of Cyrene geminal diol (hereafter 'geminal diol') when mixing Cyrene with water.

This work covers the following three main themes:

Spectroscopic analysis of Cyrene: specific focus was put on the carbonyl group and C-H vibrations. Mid-IR and Raman spectroscopy form the central backbone of this investigation. Ab initio calculations, putting forward different structural models, were performed to give more insight in the obtained results. Specifically it will be shown that the occurrence of a double carbonyl group in the IR spectrum of pure Cyrene is likely due to the formation of dimeric/oligomeric structures and not to the potential occurrence of Fermi resonance.

Analysis of Cyrene-water interaction: The system was investigated by ^{1}H NMR and ^{13}C-NMR spectroscopy allowing for the determination of the relative ratios of Cyrene, geminal diol and (by calculation) the remaining unreacted (free) water. DSC, DLS, and SAXS analysis were performed in order to probe for the potential occurrence of larger ordering extending beyond the molecular scale. It will be shown that hydrogen bonding is key to the many unusual observations.

Study of the system Cyrene/Geminal diol/Water as a solvent: here it is shown that the ternary Cyrene/gem diol/water mixture can effectively function as a switchable hydrotrope, increasing the solubility of selected pharmaceuticals up to 10000-fold, but equally as a chameleon solvent, then leading to more modest, yet still significant, increases in the solubility in the order of 9-fold.

1.2 Green Chemistry

With the continued increase in population numbers and the so created growing demand for consumer, personal care and medicinal products, the need for a sustainable manufacturing and economy as a whole is becoming paramount.[1] Industrial production requires the use of large amounts of solvents many of which are toxic. Estimations indicate a consumption of ~20 million tons per year.[2] The loss of volatile organic compounds to the atmosphere and a pertinent practice of burning solvents at the end of their life cycle, are major causes of pollution. Many of these solvents contain nitrogen and sulfur heteroatoms aggravating even further the problem as NO_x and

SO_x compounds are formed upon incineration. In this light the development of new solvents/chemicals combining a high performance with a low environmental foot print is vital. The 12 green chemistry principles developed by Paul Anastas and John Warner, are listed in a reworded fashion in table 1.1, are a very valuable guide to the development of sustainable products or processes.[3] In very general terms the sustainability of a solvent concerns not only its toxicity but also the method in which it is made in the first place.

Table 1.1 The 12 principles of Green Chemistry.

Prevention
Prevention of waste is better than treating or cleaning it up afterwards
Atom Economy
All materials used in synthetic schemes should be incorporated in the final product.
Less Hazardous Chemical Syntheses
Wherever feasible the production of materials should be designed such as to use and generate compounds displaying little or no toxicity to human health and the environment.
Designing Safer Chemicals
Chemical products should not only display the desired functionality but also be non-toxic
Safer Solvents and Auxiliaries
The use of auxiliary substances (e.g. solvents, separation agents, etc.) should be minimized
Design for Energy Efficiency
Processes should be designed to limit their energy consumption. In this light working at reduced temperatures and pressures is recommendable.
Use of Renewable Feedstocks
Thought should be given to the use of feedstocks with renewable ones being considered first
Reduce Derivatives
Chemical derivatization (e.g. the use of blocking groups, protection and deprotection...) should be avoided whenever possible as to limit the amount of waste generated
Catalysis
The use of catalysts should be preferred over stoichiometric reagents
Design for Degradation
Chemical products should be designed such that they biodegrade easily
Real-time analysis for Pollution Prevention
Analytical methodologies should also include the monitoring of toxic intermediates and gases which may end up in the environment at some stage of the process
Inherently Safer Chemistry for Accident Prevention

In developing a chemical process the nature of the starting compounds, and the reagents, should be chosen such that the occurrence of chemical accidents are limited.

For these reasons particular emphasis is being put on the use of simple water, bio-based solvents and supercritical fluids – all of which can be benign in their manufacturing and operation. Many of these solvents have similar or even enhanced performances compared to traditionally used solvents in industry.[4,5] In this respect a notable example is dihydrolevoglucosenone (Cyrene), which could serve as a rare eco-friendly alternative for toxic dipolar aprotic solvents such as N-methylpyrrolidone, N,N-dimethylformamide and N,N-dimethylacetamide (Figure 1.1.).[1] Cyrene's renewable nature and absence of mutagenicity/toxicity make it particularly attractive as a solvent.[1]

1.3 Solvent properties

Solvents serve many proposes amongst which (not limiting):

a) conduct reactions, then predominatly dissolving the different compounds
b) assist in separation processes, recovering the desired products
c) transporting different materials throughout extensive chemical process cycles
d) stabilize reaction intermediates
e) shifting equilibria

Their physical properties, like hydrogen bonding ability and boiling point, can affect the yield of the processes. Frequently solvents serve to dissolve chemicals in which case the nature of the interaction between solvent and solute becomes very important.[4] Typically the rule of thumb is that like-dissolves-like and polarity is thus an important parameter to consider. Molecules with a permanent dipole are call 'dipolar'. Notably the connotation 'apolar' is rarely used to describe solvents as phenomena like polarizability have to be take in account.[5] Additionally solvents can also be classified as aprotic or protic. In contrast to protic solvents, aprotic solvents have no dissociable hydrogen atoms. Intermolecular solute/solvent interactions are often highly complicated in nature and difficult to determine in a quantitative fashion.[6]

The effect of solvents is also very visible in analytics where, for instance, the position and intensity of the absorption bands in UV/VIS, IR, NMR, and ESR spectroscopy, are often significantly solvent-dependent.[7] This is often related to differential solvation of reactants and products or the different physical absorption of electromagnetic radiation. The degree of the former depends mainly on the intermolecular forces between the solute and the surrounding solvent molecules.[8,9] Nowadays many parameters are available to describe the principal characteristics of solvents. The best way forward to establish the polarity of a given solvent depends on the balance of several factors like electrostatic, inductive, dispersive, charge-transfer and hydrogen bonding forces.[5,10] Also many physical and chemical properties like the dielectric constant, the capacity to donate/accept electron pairs, and the ability to stabilise charges are of considerable importance to describe correctly the polarity of solvents.[5] The effect of solvents on chemical reactions can very often be understood in terms of the so-called solvent polarity.

1.4 Regular solutions

The term "regular solution" was proposed by Hildebrand, these solutions exhibit specific interactions between molecules (such as association, dipole interaction or hydrogen bonding). In the regular solutions "the random mixing of molecules arising from thermal energy which overcomes the difference in mutual molecular forces".[11] For a regular solutions the entropy of mixing is not equal to zero but it depends on composition. An increase of entropy is not strongly influenced by the molecular size but, instead the heat of solution is proportional to the molar volume.[11] The mixing of two substances is accompanied by an increase in entropy and the value of the free energy change depends upon the enthalpy factor.[12]

Hildebrand and Scott proposed the relation:

$$\Delta H_m = V_m \left[\left(\frac{\Delta U_1}{V_1}\right)^{\frac{1}{2}} - \left(\frac{\Delta U_2}{V_2}\right)^{\frac{1}{2}} \right]^2 \varphi_1 \, \varphi_2 \qquad \text{[Eq.1.4.1]}$$

Where ΔH_m is the enthalpy of mixing, V_m is the volume of mixture, ΔU is the internal energy change on vaporization, V is molar volume, and ϕ is the volume fraction of the component.[12] The term ΔU/V is the energy of vaporization per unit volume for a component and is a measure of the amount of energy necessary to overcome all the intermolecular forces holding the molecules together in a unit volume of substance and is called cohesive energy density.

It is possible rearrange the equation in the following manner:

$$\frac{\Delta H_m}{(V_m \ \varphi_1 \varphi_2)} = (\delta_1 - \delta_2)^2 \qquad \text{[Eq.1.4.2]}$$

Where $\delta = \left(\frac{\Delta U}{V}\right)^{\frac{1}{2}}$

δ is called the solubility parameter measured in $(cal/cm^3)^{1/2}$. From the previous equation it follows that two substances are miscible if $(\delta_1 - \delta_2)$ is small or zero. In theory is possible predict if two different substances are miscible from their values of δ. Thereby, δ is a parameter of intermolecular interaction of an individual liquid. It is possible calculate the value of the solubility parameter in many ways, for instance from the calorimetric heats of vaporization using the relation:

$$\delta = \left(\frac{\Delta H^v - RT}{V^l}\right)^{\frac{1}{2}} \qquad \text{[Eq.1.4.3]}$$

where ΔH^v is the heat of vaporization and V^l is the molar volume of the liquid or from the value of vapour pressure using the relation: [13]

$$\delta = \left[\frac{(\Delta H^V_{app} - RT)Z}{V^l}\right]^{\frac{1}{2}} \qquad \text{[Eq.1.4.4]}$$

where ΔH^V_{app} is the apparent heat of vaporization and Z is the compressibility factor.[13]
However, the theory of regular solution from which δ is derived, has many restrictions.[14] In fact, this is only valid if dispersion forces interact between molecules (where the energy of contacts between heterogeneous molecules is a geometric mean value of the energy contacts between the

molecules).[15,16] The theory cannot predict the behaviour of polar substance or specific interaction like those between functional groups in a polymers mixture. Furthermore, it does not take in account the volume change on mixing.[17] Other tools have been developed to better describe the behaviour of solutions, particularly in order to predict the solubility between two substances. For instance, in 1966 Hansen proposed that the cohesive energy E can be divided into three types of contribution, dispersion interaction, polar interaction, and hydrogen bonding. These can be written as:

$$E=E_d+E_p+E_h \qquad \text{[Eq.1.4.5]}$$

Where E is the total cohesive energy, E_d is the dispersion contribution, E_p is the polar cohesion energy, and E_h is the hydrogen bonding cohesive energy. Dividing for the molar volume of solvent V_1 it possible write the following equation:

$$E/V_1=E_d/V_1+E_p/V_1+E_h/V_1$$

Which can be rewritten as

$$\delta = \delta_d^2 + \delta_p^2 + \delta_h^2 \qquad \text{[Eq.1.4.6]}$$

where δ is the total solubility parameter, the others are the solubility parameter due to the corresponding contributions to the cohesive energy.[18]

1.5 Dimroth and Reichardt's *E*T(30) and Kamlet-Taft's solvatochromic parameters

The polarity of a solvent is determined by its solvation behaviour, which depends on the action of the intermolecular forces interacting between solvent and solute.[19] For the estimation of solvent polarities it is necessary to use empirical parameters obtained for certain standard substances used as probes, by the measurement of some suitable property that exhibits a large solvent-sensitivity.[20]

The term solvatochromism is used to describe the pronounced change in position of a UV visible absorption band following a change in the polarity of the medium.[19] It was found that in the absorption spectra of a substance, the position the shape and the intensity of the absorption band can vary, depending on the nature and polarity of the solvent. Dimroth and Reichardt's *E*T(30) and Kamlet and Taft's parameters are based on the solvent-induced shifts of the lowest energy absorption bands of certain solvatochromic indicators in the ultraviolet-visible spectral region.[20] The ET (30) scale developed by Reichardt is based on the spectroscopic behaviour of this betaine indicator dye, 4-(2,4,6-triphenylpyridinium)-2,6-diphenylphenoxide (ET-30).[21,22] The values of *E*T(30) are obtained from the maximum wavenumber of the longest wavelength charge transfer absorption band of the betaine indicator in dilute solution in the solvent, it shows a very wide blue-shift effect in solvents with increasing polarities. Occasionally, normalized values (E_T^N) are reported, where the zero point of the scale is defined by the shift in tetramethylsilane and a value of one for the shift in water.[18] Kamlet and Taft were the first to develop a multiparameter correlation equation based on solvatochromic measurements.[23,24,25] "Their π* or dipolarity-polarizability scale is based on the solvent-induced shifts of the frequency maxima of the π→π* transitions of several indicator dyes, where the values are normalized so that the π* of cyclohexane is 0 and that of dimethyl sulfoxide (DMSO) is 1."[25] This scale is presumed to represent solute-solvent interactions in the absence of strong forces such as hydrogen bonding or ion dipole interactions.[25] In general, the Kamlet–Taft formalism for describing solvent parameters is given by:[25]

$\nu_{max} = \nu_0 + s\pi^* + a\alpha + b\beta$ [Eq.1.5.1]

where ν_{max} is the is the frequency of the maximum absorption of the indicator dye in the solvent of interest. The intercept ν_0 and coefficients s, a, and b are determined by the nature of the indicator dye. π^* represents the dipolarity-polarizability term, α is the hydrogen bond donor ability and β is the hydrogen bond accepting ability. In order to avoid the influence of a specific effect between on single dyes and the solvent, in the Kamlet-Taft scale the values normally used are calculated from an average of different dyes.
Nowadays the values of these parameters are available for many substances, which can be very useful to predict the solubility between substances.[26]

1.6 Cyrene and Cyrene/Geminal diol/Water

Dihydrolevoglucosenone (Cyrene) is a new established bio-based dipolar aprotic solvent (Figure 1.1.). Conveniently it can be synthesised in only two simple steps from biomass: a) converting first cellulose into levoglucosenone at elevated temperature using an acid catalyst and b) hydrogenating the aliphatic double bond in the presence of a catalytic amount of Pd creating dihydrolevoglucosenone, also known as 'Cyrene'. As such the production of this solvent displays a very low ecological footprint, which adds significantly to its economic viability.[1] (Scheme 1.1).[27] The chemical process to the formation of Cyrene is illustrated in scheme 1.1.

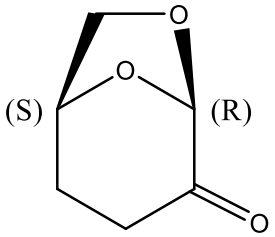

Figure 1.1 Structure of (1S,5R)-6,8-Dioxabicyclo[3.2.1]octan-4-one (Cyrene)

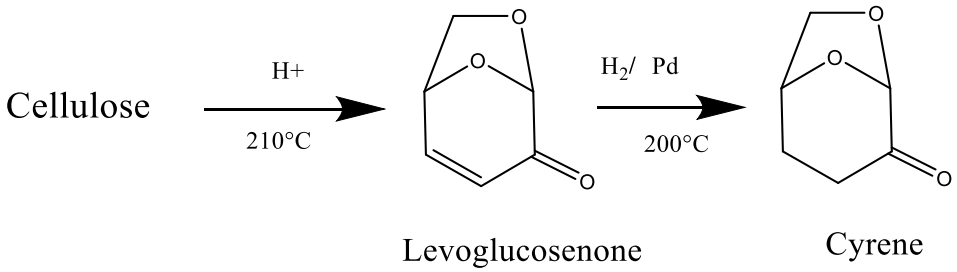

Scheme 1.1 The synthesis of Cyrene from biomass/cellulose.

Table 1.2 shows the more relevant physical properties of Cyrene. The Kamlet–Abboud–Taft parameters for Cyrene indicate that this solvent is aprotic with its hydrogen bond donor (HBD) ability (α) being zero. Cyrene shows a similar π* value to those of highly dipolar aprotic solvents, but with a slightly lower β value, the latter being an indicator of hydrogen bond accepting ability.[1] Table 1.2 also reports the value of the Hildebrand solubility parameter, which defines a solvent's affinity to dissolve a solute. Generally a solute is soluble in solvents having a similar solubility parameter.[28] It is possible to locate a solvent in the ''Hansen space''. This is a three-dimensional representation displaying the dispersion (δd), polar (δp) and hydrogen bonding (δh) interactions as the xyz axes. When two solvents are situated close in the Hansen space it can be said that they exhibit similar solubilising properties. Considering this parameter the closest solvent in the Hansen space to Cyrene is NMP (N-Methyl-2-pyrrolidone). [1] In spite of the higher boiling point of Cyrene (~203-210 °C), its many beneficial properties make it a very interesting solvent and notably a rare bio-based dipolar aprotic.[1] As many solvents are presently being restricted and banned by Reach, and related organizations worldwide, Cyrene is receiving significant industrial interest as it would allow potentially for the substitution of a range of Reach-restricted repro-toxic, dipolar aprotic solvents, such as N-methylpyrrolidone (NMP), N,N-dimethylformamide (DMF) and N,N-dimethylacetamide (DMAC).[1]

Table 1.2 Kamlet-Abboud-Taft parameter for Cyrene.

	Cyrene	NMP	Cyclohexanone
E_T^N	0,333	0,355	0,281
α	0,00	0,00	0,00
β	O,61	0,75	0,58
Π*	0,93	0,90	0,71
δ_D/MPa^{0,5}	18,8	18,0	17,8
δ_p/MPa^{0,5}	10,6	12,3	6,3
δ_H/MPa^{0,5}	6,9	7,2	5,1

Moreover the combination of Cyrene and water, discussed in this manuscript and submitted for publication, imparts even tuneability to particular applications. More specifically, combining Cyrene with water leads to the formation of defined amounts of geminal diol. The so created ternary system has been thoroughly characterized displaying unusual properties in terms of the equilibrium constant (Keq), the density and the viscosity. In essence the newly formed geminal diol is an amphiphilic molecule which can act as both a switchable hydrotrope and a chameleon solvent. The term switchable is used while the simple addition of water to Cyrene creates geminal diol in a reversible manner. The mechanism of hydrotropy has long been misunderstood and a rigorous theory was only recently developed linking hydrotropic dissolution to a non-specific association of the hydrotrope on the solutes.[29,30,31,32]

1.7 Fermi resonance

A possible explanation for the observation of two separate carbonyl groups in the IR spectrum lay in the occurrence of Fermi resonance.[33,34] Infrared or IR spectroscopy is an analytical technique which is based on the interaction between electromagnetic radiation and matter.[35] When an organic molecule is subjected to infrared light with a frequency in between 10,000 and 100 cm^{-1}, the energy comprised in the infrared light is converted into vibrational energy. In a spectrometer the molecule is irradiated with a wide range of infrared frequencies. Different functional groups will absorb IR light of different frequencies hence creating an IR spectrum.[35]

Although the infrared spectra of polyatomic molecules involve vibrational transitions along with rotational transitions, the peaks in the infrared spectrum could be assigned as a fundamental vibrational transition only. This is especially true for the case of polyatomic molecules where the rotational fine structure is lost because to the intermolecular interactions. In a real IR spectrum, the motion of nuclei cannot be isolated from the motion of other closely surrounding nuclei in the molecule, and for this reason, the characteristic absorption of a particular functional group in a molecule can be assigned only to a range of characteristic frequencies in the infrared spectrum. Hence, in the low-resolution IR spectrum the frequency bands are in a first approximation due to vibrational transition only.[35] Vibrational spectroscopy has as an objective the analysis of molecular vibrational transitions between different states. For this purpose it is necessary to understand how the relevant energy levels are organized and which therein are allowed. In order to analyze the

vibrations of a molecule, it is helpful to determine the number of degrees of freedom available to vibration. To represent the movement in space of a molecule consisting of N atoms, we need to use 3N coordinates. These coordinates represent the 3N degrees of freedom necessary to describe the translational motion, rotational and vibrational modes in a molecule. To describe the translational motion of a molecule we need three coordinates. To describe its rotational motion and the orientation in the space, two or three coordinates are needed depending on whether the molecule is linear or nonlinear. The vibrational motion concerns the reciprocal displacement of the atoms in the molecule. The degrees of vibrational freedom are equal to the difference between the total degrees of freedom and the sum of the rotational and translational ones, so 3N- (3 + 2) or 3N- (3 + 3). These also are the normal modes of vibration of the molecule. The normal coordinates correspond to the actual vibrational modes that the molecule will undergo.[36] It can also be helpful to use other coordinate systems to describe adequately the vibrational motion of a molecule. One of these uses internal coordinates involving bonds and angles.[35] In a molecule, it is possible to distinguish between different types of vibrational movements. The vibration stretching indicated with the letter ν, in which we have a modification in the length of the bonds, can be of two types, symmetrical and asymmetric.

The vibration bending (δ) is another type of vibration in which a change to the bond angles occur. We can distinguish four types of bending:[35] 1) rocking, 2) scissoring, 3) twisting and 4) wagging

The vibrations of a molecule set up a potential called force field, and the simplest force field model is the harmonic oscillator.

To describe the energetic vibrational state of a molecule one needs to solve the Schrödinger equation. For instance, in considering the simplest force field model, the harmonic oscillator, for a simple diatomic molecule (See Figure 1.2.) the potential energy can be written down as a Taylor series (equation 1.7.1.):[37]

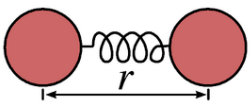

Figure1.2 Typical model for the harmonic oscillator.

$$V_{(x)} = V_{(0)} + \left(\frac{dV}{dx}\right)_0 x + \frac{1}{2}\left(\frac{d^2 v}{dx^2}\right)_0 x^2 \qquad \text{[Eq.1.7.1]}$$

$$x = r - r_e$$

Where r_e is the bond length when the potential energy in the molecule is at a minimum. The first two terms are then both equal to 0 making that the remaining last term could be interpreted as a force constant. Then the harmonic approximation of the potential energy reduces itself to:

$$V_{(R)} = \frac{1}{2} K x^2 \qquad K = \left(\frac{d^2 v}{dx^2}\right)_0 \qquad \text{[Eq.1.7.2]}$$

The curve of the potential energy is described as a parabola. Introducing this form of the potential energy in the Schrödinger equation gives equation 1.7.3.[38]

$$-\frac{\hbar^2}{2\mu}\frac{d^2\psi}{dx^2}+\frac{1}{2}Kx^2\psi = E\,\psi \qquad \text{[Eq.1.7.3]}$$

Where

$$\mu = \frac{m_1 m_2}{m_1+m_2}$$

and the solution of the Schrödinger equation (converted in wavenumber cm^{-1}) is then: [39]

$$G(v)=\left(v+\frac{1}{2}\right)\tilde{\nu} \quad \text{where}$$

$$\tilde{\nu} = \frac{1}{2\pi c}\left(\frac{K}{\mu}\right)^{\frac{1}{2}} = \frac{\omega}{2\pi c} \qquad \text{[Eq.1.7.4]}$$

$$\omega = \left(\frac{K}{\mu}\right)^{\frac{1}{2}}$$

v is the vibrational quantum number and can have only integer values 0,1,2, 3 etc. The state at $v = 0$ corresponds to the ground-state of the vibrational energy. From this expression we can see that the energetic levels of a harmonic oscillator are uniformly separated from one another. In reality, the harmonic oscillator model is only an approximation and in the real world the molecules do not truly obey Hooke's law.[40]

It follows that Hooke's law restoring force of nuclei is not proportional to their displacement, especially when concerning large vibrational amplitudes. Moreover this model does not consider the breaking of the bond nor any repulsion between the nuclei. A more appropriate model uses the equation of Morse. This is another empirical expression to describe the form of the potential energy for the molecular vibrations (equation 1.7.5):[41,42]

$$V(x)= D_e\,(1De^{-ax})^2 \qquad \text{[Eq.1.7.5]}$$

where D_e is the dissociation energy and 'a' a particular constant for the molecule under consideration. Using this equation to solve the Schrödinger equation, the shape of the vibrational energy levels become:

$$G(\nu)= \left(\nu+\frac{1}{2}\right)\tilde{\nu} - \left(\nu+\frac{1}{2}\right)^2\tilde{\nu}\,x_e \qquad \text{[Eq.1.7.6]}$$

Where

$$x_e = \frac{a^2\hbar}{2\mu\omega} = \frac{\tilde{\nu}}{4D_e}$$

Here X_e represents the anharmonicity constant for bond stretching vibration, and $\tilde{\nu}$ is the oscillation frequency. One result of the use of this form of potential is that with increasing ν the different vibrational levels become closer together.[43] (See Figure 1.3.)

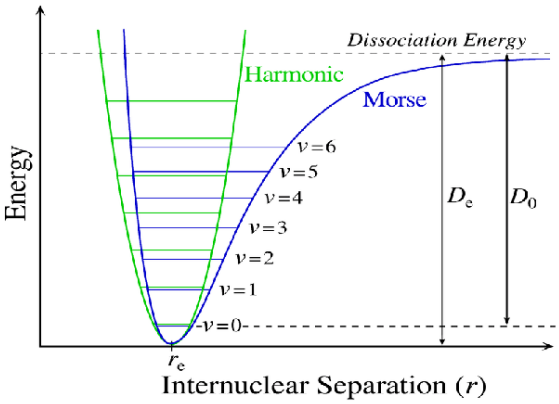

Figure 1.3 Morse potential compared with the one for the pure harmonic model.

For molecules with multiple atoms (>2) many different vibrational modes are possible. The minimum number of displacement coordinates R_i to describe the changes of nuclei configuration needed is defined as 3N-6 displacement. It must be stressed that the real bonds in the molecules are not elastic and that there is always a certain degree of anharmonicity present. One of the effects of anharmonicity is that normal vibrations are mixed, it perturbes the energy levels from their harmonic position. Taking into account anharmonicity, the potential energy acquires the following complex form (equation 1.7.7): [44]

$$V=\frac{1}{2!}\sum_{i,j} f_{i,j}\ R_iR_j+\frac{1}{3!}\sum_{i,j,k} f_{i,j,k}\ R_iR_jR_k+\frac{1}{4!}\sum_{i,j,k,l} f_{i,j,k,l}\ R_iR_jR_kR_l+\ldots\ldots \quad \text{[Eq.1.7.7]}$$

The first term in this equation 1.4 (number) is the quadratic term of the harmonic force field. The second and third terms correspond to cubic and quartic contributions to the force field. The solution of the Schrödinger equation for a molecule in which all vibrations are not degenerative is (equation 1.7.8):

$$\sum_i G(V_i)=\sum_i \tilde{\nu}\left(\nu_i+\frac{1}{2}\right)+\sum_{i\le j} x_{ij}\left(\nu_i+\frac{1}{2}\right)\left(\nu_j+\frac{1}{2}\right)+\ldots\ldots \quad \text{[Eq.1.7.8]}$$

Not all vibrations are active in IR spectroscopy. For the harmonic model, it was found that the quantum number changes by one, but also the dipole moment of the molecule must change in the course of an allowed transition.[44] Therefore, a particular vibrational mode of a polyatomic molecule will be active in the infrared, if the molecule's dipole changes in a normal mode vibration. Classically the dipole moment of a molecule is determined as follows:

$$\mu_x=\sum_i q_i x_i$$

$$\mu_y=\sum_i q_i x_y \qquad \text{[Eq.1.7.9]}$$

$$\mu_z=\sum_i q_i x_z$$

Here all atoms are considered to have a partial charge, and for those atoms which are chemically equivalent the assumption is that they have the same charge. The displacement of the atoms in a normal mode of vibration is then only considered when there is an actual change in the dipole moment of the molecule. Therefore it is imperative to have in depth knowledge on the symmetry of the molecules. Indeed possible IR and also Raman active bands in the spectra relate directly to

the symmetry of the molecule.[45] However to understand Fermi resonance phenomena it is not strictly necessary to delve deep into group theory but, it suffices to keep a few elementary principles in mind. For all the allowed transition, the vector dipolar moment must be (equation 1.7.10):

$$\mu = \int \psi_f^* \hat{\mu} \psi_i \, d\tau \quad \text{and} \quad \Delta v = \pm 1 \qquad \text{[Eq.1.7.10]}$$

where ψ_f^* is the wave function of a final state of transition and ψ_i is the wave function of the initial state of the transition and the vibrational quantum number has to change with 1.

1.8 Selection rules and types of transitions

The general selection rules state that: 1) a vibrational transition is IR active if there is a variation of the electronic dipole moment of the molecule during vibration and 2) the only permitted vibrational transitions are the ones with $\Delta v = \pm 1, \pm 2, \pm 3, ...$

The fundamental transitions are those that take place between the ground state and the vibrational first excited level (i.e. $v = 0 \longrightarrow v = 1$). The corresponding band is called the fundamental band and is usually strong. The transition from the ground state to the excited state $v = 2$ is called the second harmonic, the one between the ground state and the excited state $v = 3$ the third harmonic and so on. The corresponding bands are called the first overtone, the second overtone, the third overtone etc.

The intensity of such overtones is evidently significantly lower than the fundamental bands becoming ever weaker with increasing quantum number of the vibrational excited level. It is also possible to have transitions from one excited vibrational state to another one with a higher energy. These are called “hot transitions” and the corresponding band is called a “hot band”. Such phenomena complicate appreciably the molecular spectra.[46]

Other bands are called combination bands and derive from the transitions between a fundamental state and a state where more normal modes are excited. In general they are significantly weaker than the related fundamental bands. However, as previously stated, one of the effects of anharmonicity is that the normal vibrations are mixed and that the energy levels are perturbed from their harmonic position. All the perturbation is rigidly restricted by symmetry. In a polyatomic molecule it may though happen that two vibrational energy levels, belonging to different vibrations, or being the result of a combination of vibrations with the same symmetry and nearly the same energy, may give rise to an unusually large perturbation. If then such perturbation involves actually a fundamental band and an overtone or a combination of bands, one speaks of Fermi resonance. The Fermi resonance is a kind of anharmonic resonance. It is named 'type one' if a fundamental and an overtone band are involved and 'type two' if a fundamental and a combination of bands are involved. The quantum mechanics behind this interaction are complex; in laymen's terms it can be said that two energy levels repel each other with the one at highest energy being pushed up and the one lower in energy being pushed down.[47] The macroscopic effect of this interaction may show up in both IR and Raman spectra as a doublet band in a region where only one band is expected. Normally the fundamental band has the strongest intensity and is at the highest energy. Conversely the Fermi resonance peak is significantly smaller and it is situated at lower energy.

The magnitude of the perturbation between the two energy levels depends on the value of the matrix element $W_{i,j}$ of the perturbation function W (equation 1.7.11):[48]

$$W_{i,j} = \int \psi_i^0 \quad \hat{W} \quad \psi_j^{0*} d\tau \qquad \text{[Eq.1.7.11]}$$

Where the ψ_i^0 and ψ_j^0 are the zero approximation eigenfunctions of the two vibrational level that perturb each other.[49]

The magnitude of the shift between the levels can be obtained by applying the first order perturbation theory. For instance, considering just the case of two levels with unperturbed energies E_i^0 and E_j^0, and with ΔE being the shift of the levels, it is possible to write the following secular determinant:

$$\begin{vmatrix} E_i^0 - \Delta E & W \\ W & E_j^0 - \Delta E \end{vmatrix} \qquad \text{[Eq.1.7.12]}$$

Solving the determinant we get:

$$\Delta E = \left[(E_i^0 + E_j^0)/2\right] \pm (4W^2 + \delta^2)^{\frac{1}{2}}/2 \qquad \text{[Eq.1.7.13]}$$

Where δ is the energy of separation E_i^0- E_j^0 of the unperturbed level. If δ is large compared with 2W, a condition which is met when the levels are well separated, the equation becomes:

$$\Delta E \approx \left[(E_i^0 + E_j^0)/2\right] \pm \left[\left(\frac{\delta}{2}\right) + \frac{W^2}{\delta}\right] \qquad \text{[Eq.1.7.14]}$$

In the case of the Fermi resonance the wave functions ψ_i and ψ_j of the perturbed states are a linear combination of the wave functions ψ_i^0 and ψ_j^0

$$\psi_i = a\psi_i^0 - b\psi_j^0 \qquad \text{[Eq.1.7.15]}$$

$$\psi_j^0 = b\psi_i^0 + a\psi_j^0$$

Here a and b are numerical coefficients.[50] Often one of the effects of a strong mixing of the vibrational levels is that bands of similar intensity can be observed in both the Raman and the IR spectra.[51] Exemplary are the Raman and IR spectra of CO_2.

In the light of the above, it is in principle possible to obtain from the IR spectra all the information necessary to calculate the Fermi coupling constant. As such the (non)-existence of Fermi resonance in the IR spectrum of Cyrene can be proven/disproven.

Chapter 2: *the spectroscopic properties of Cyrene*

Chapter 2

2.1 Spectroscopic (IR/NMR) characterisation of the Cyrene

2.1.1 Liquid phase infrared spectroscopy and Karl Fisher titration

The IR spectrum of neat double-distilled Cyrene shows two distinct carbonyl group peaks, notably at 1742 cm^{-1} and 1725 cm^{-1}, where only one is expected. This can be adequately inferred from Figure 2.1, showing the overall IR spectrum, and Figure 2.2, showing a close up of the carbonyl stretch region.

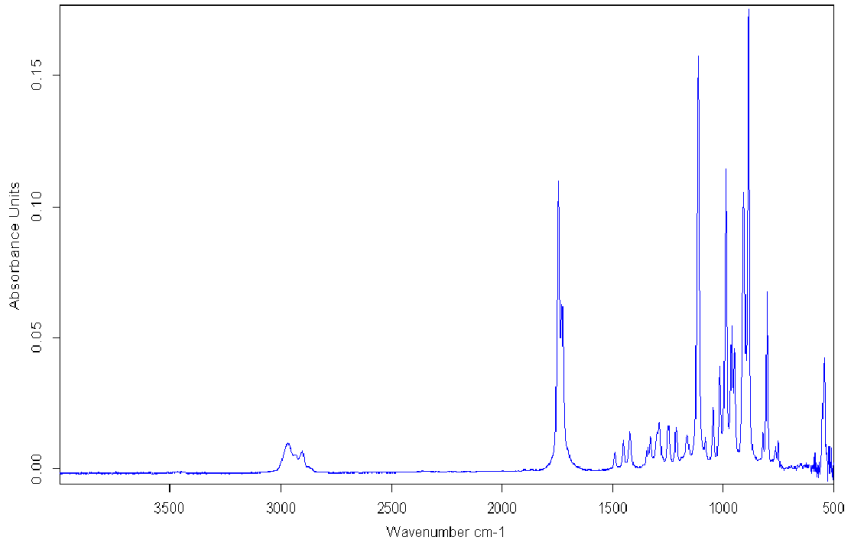

Figure 2.1 FT-IR of pure Cyrene at room temperature.

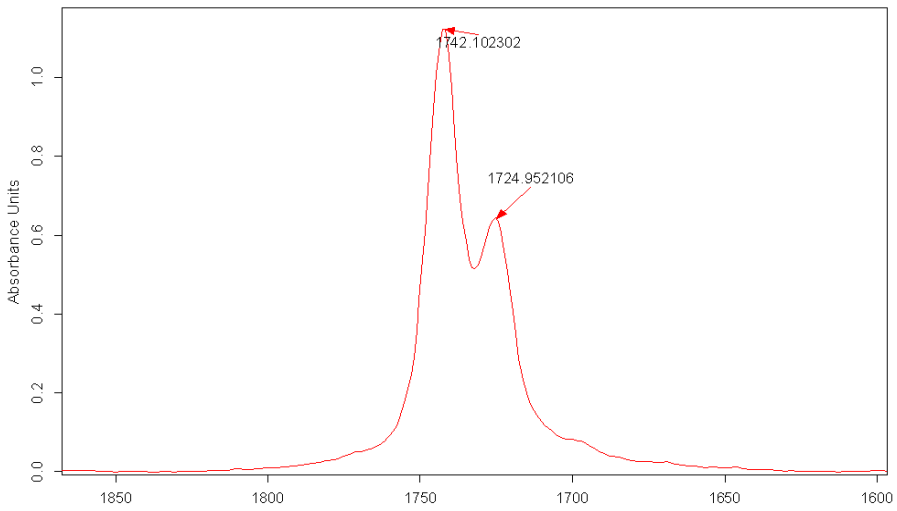

Figure 2.2 FT-IR of pure Cyrene at room temperature – *close up of the carbonyl region.*

The presence of the two distinct carbonyl stretches in the IR spectrum was consistently found and in no way depended on the batch of dihydrolevoglucosenone. Also the relative peak intensities never changed.

However, based on the molecular structure of Cyrene, only a single intense carbonyl peak would have been expected in this region.[52] The infrared absorption band arising from the C=O stretching vibration has been studied more extensively than any other making that a significant amount of information is available on the factors influencing its frequency and intensity.[52] The frequency of the carbonyl absorption is determined almost entirely by the nature of its immediate chemical environment. The overall configuration of the molecule is significantly less important in this respect unless the molecule under consideration displays phenomena like dimerization, keto–enol tautomerism or some kind of resonance effect.[52,53] As such considerable amount of data can be found in the literature describing the influence of the nature, intensity and position of this band.[52] It is also known that the frequency of the carbonyl group is significantly influenced by the chemical environment around it. For instance, its position depends on the nature of the solvent used.[54-57] In the literature many explanations can be found for the occurrence of two peaks in the carbonyl region of the IR spectra [52,58,59] including, but not limited : a) the opening of the molecule with the resultant formation of rotational isomers b) the fast opening and closing of the ring bond (as occurs in sugars) [60]c) the presence of carbonyls with two different chemical environment (caused for example by molecular aggregation)[52] d) complex formation e) the presence of two different molecular configurations[58,59] f) the formation of a dimer or oligomer g) a dual band being the result of some kind of coupling (for instance a Fermi resonance).[52]

In a first instance, a careful check was performed to establish whether particular impurities were present in Cyrene. Due to the nature of Cyrene manufacturing procedure, small quantities of Pd could well form a complex with the carbonyl group(s), causing the splitting of the relative band.[61] While double distilled Cyrene only holds only ppm levels of Pd this was found rather implausible. Nonetheless to rule out possible complexation between Pd and Cyrene's carbonyl group, Cyrene made by Raney Nickel was also examined showing again the double carbonyl group. It was also verified that crude Cyrene (as received) and further in-house purified Cyrene (further distillations) gave identical IR spectra. It was tested whether the deliberate addition of $PdCl_2$ (1.229×10^{-4} mol) to a defined amount of Cyrene (0.019511 mol) would further affect the carbonyl region in the IR spectrum, and most notably the relative ratio of the two carbonyl peaks. The so additional IR spectra all exhibited the same shape for the carbonyl band with the same relative intensity of the two carbonyl stretches, suggesting that the nature of this phenomenon is due to causes other than complexation between Pd and the carbonyl group.

The presence of water was also considered as a potential reason for the occurrence of the double carbonyl group. To shed more light on this a Karl Fischer titration was carried out on neat, as received, Cyrene and an average of 0.33 wt% water was found present in the samples. The Karl Fisher titration report is shown in Figure 2.3.

The Karl Fischer reaction for water determination follows the equation:

$$H_2O + I_2 + [RNH]^+ SO_3CH_3^- + 2\ RN \rightarrow [RNH]^+ SO_4CH_3^- + 2\ [RNH]^+ I^- \qquad \text{[Eq. 2.0]}$$

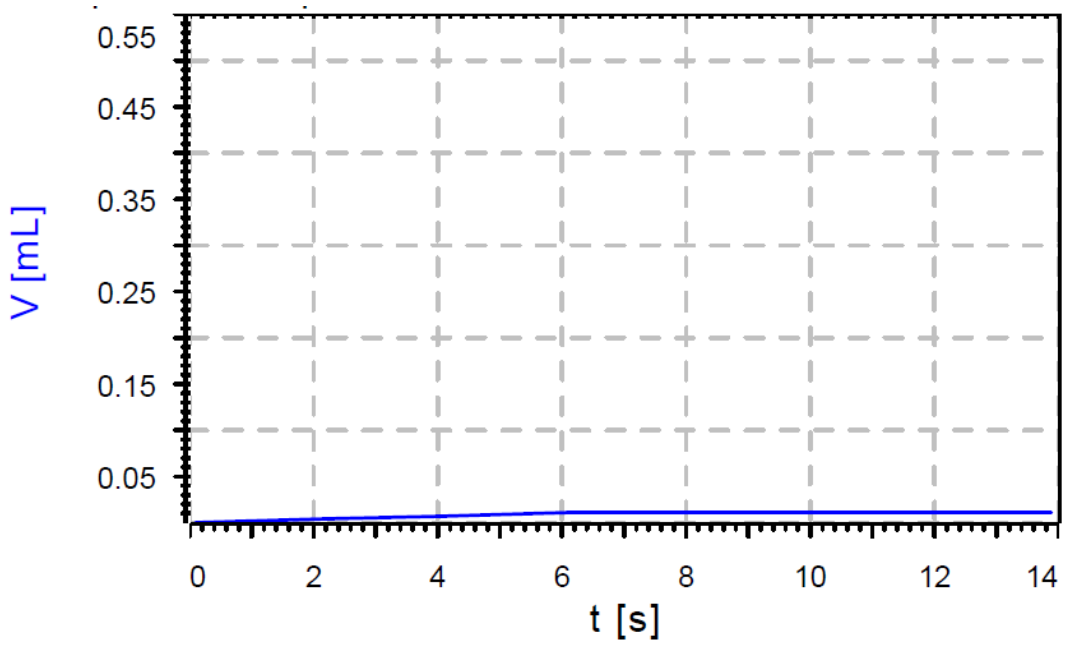

Figure 2.3 Karl Fisher titration on neat Cyrene shows the volume of titrant solution (ordinate) in function of time in seconds (abscissa).

Thereby RN is a base and the experiment is generally performed in methanol. In this reaction one mole of I_2 is consumed for each mole of H_2O. The presence of both aldehydes and ketones pose though problems in Karl Fisher (KF) titrations because they form acetals and ketals with conventional KF reagents.

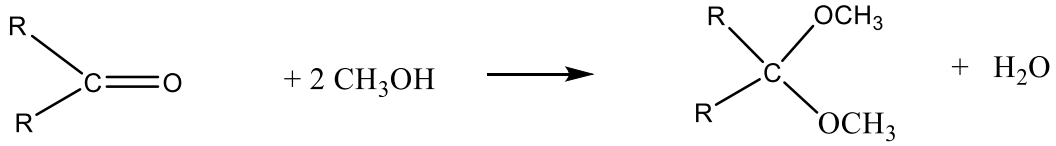

[Scheme.2.1]

Moreover as acetal/ketal formations forms water in its own right the end result is questionable as also this newly formed water gets titrated during the KF experiment. Furthermore, specifically with aldehydes another side reaction can also occur:

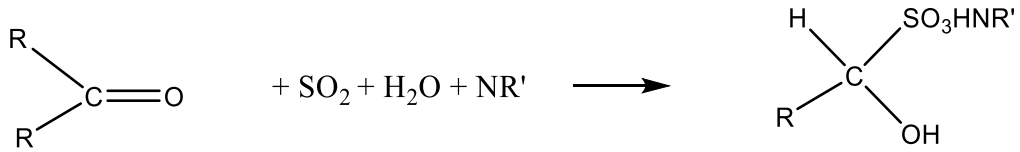

[Scheme.2.2]

In the presence of aldehydes adding the bisulfite causes a reaction in which water is actually consumed therewith underestimating the amount of water present.[62] For all the above stated reasons the titration of Cyrene was performed using HYDRANAL®, methanol free, and in the presence of a specific base which does not lead to significant side reactions.

Equally noteworthy is that the IR spectrum of neat Cyrene does not display any significant OH peak. As to the double carbonyl group the situation is actually even more complex in that the second derivative of the first carbonyl peak (the one at higher energy) reveals one single contribution but the one of the second peak reveals multiple ones. Deconvolution of the Cyrene spectra using OPUS indicated the possible presence of more than two carbonyl peaks. For the sake of clarity, and as to not complicate the situation, it must be said that the additional contributions beyond two carbonyl peaks are particularly weak making that we will not include these in the general discussion.

The distance between the maxima of the two carbonyl peaks is about 17 cm^{-1}, which is in clear excess of the applied 2 cm^{-1} resolution. This would be consistent with the assumption that the carbonyl group could be involved in intermolecular hydrogen bonding interactions.[52] Another possible explanation is the potential occurrence of two different chemical environments around the carbonyl group. This would only make sense though in case some kind of structural ordering would exist in the neat cyrene.[52] For example, the formation of dimers, trimers or other oligomers. A visual representation of how this could come about is shown in Figure 2.4.

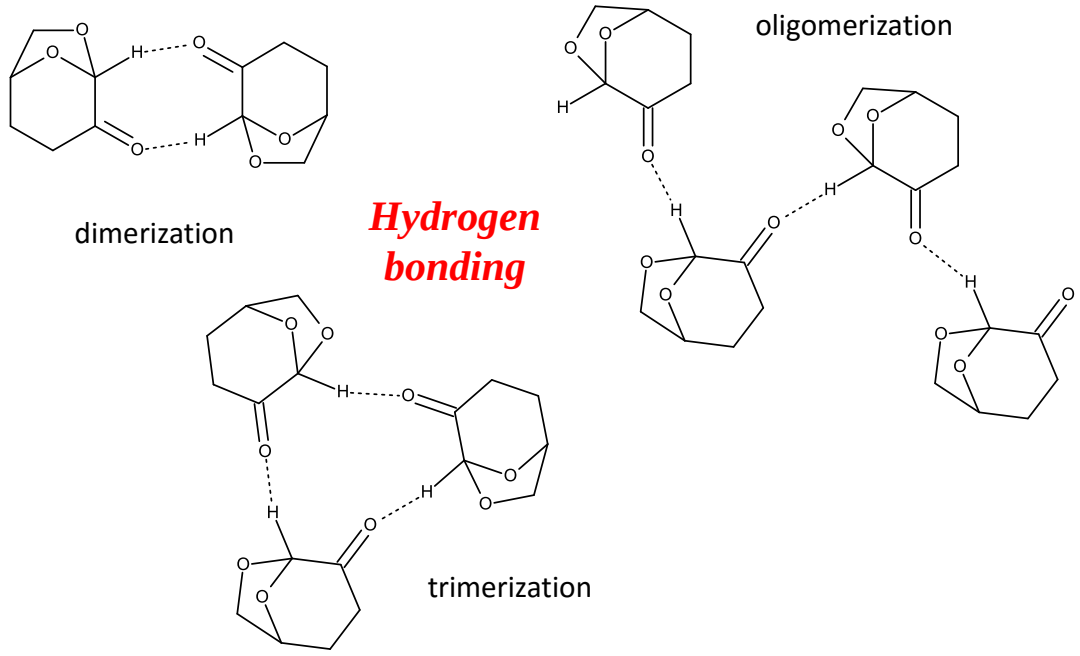

Figure 2.4 Possible intermolecular organization in neat Cyrene.

2.1.2 Variable temperature and gas phase infrared spectroscopy

In the case of Cyrene, study of the mid-IR spectra was found of limited value due to the high density of vibrational states and the low symmetry of the Cyrene molecule. Furthermore, the mid-IR region is known to allow nearly only the assignment of families of molecular structures (e.g. CH_x groups, C=O groups, C-O groups etc).[63] However, in spite of these limitations it is nonetheless possible to shed further light on the observed odd spectroscopic features in the Cyrene IR spectrum. It should be noted that the combined use of IR and Raman spectroscopy allows to probe for structural organization. More specifically the occurrence of intra- and intermolecular interactions between

different functional groups in the molecules do have a significant impact on the wavenumber of the absorption bands and their intensity.[64] Another method to verify the presence of structural organization is through FTIR (or Raman analysis for that matter) at different temperatures. Here comparison of the obtained spectra with the gas phase IR spectrum is paramount (Figure 2.5). In the case of ordering, like in dimerization or oligomerization, the relative height of the different IR signals for the carbonyl bands, should vary with changes in the temperature.[65,66]

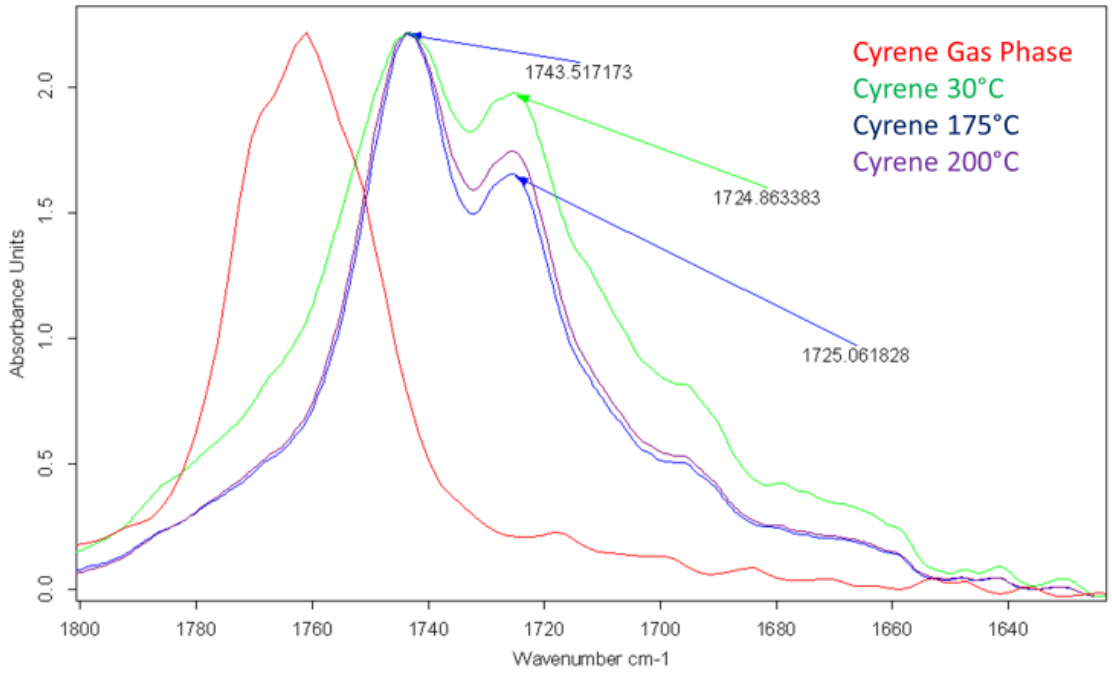

Figure 2.5 Evolution of the carbonyl IR region as a function of temperature (DRIFT at 30, 175 and 180 °C); in red the peak of Cyrene in gas phase.

The gas phase IR spectrum of pure Cyrene is shown in Figure 2.6, with a close up on the carbonyl region shown in Figure 2.7. It can be seen that under these conditions only one carbonyl peak can be identified notably the one at higher energy. Additionally, comparing the IR spectrum for both the gas and the liquid phase, the carbonyl IR peaks position in the gas phase IR spectrum occurs at a higher wavenumber. In the event that dimers, trimers or other oligomers of Cyrene exist, the expectation is such that an increase in the temperature leads to an increase in the intensity of one of the observed carbonyl peaks. Normally, and logically, this should be the band related to monomeric Cyrene. Likewise the carbonyl absorptions related to the oligomeric Cyrene structures should then decrease in intensity with increasing temperature. This behaviour relates directly to the progressive breaking of hydrogen bonds between the different Cyrene molecules leading to an ever increasing amount of monomeric Cyrene. Most interestingly though this theory does not correlate with the experimental observations temperature has no real influence on the relative heights on their relative position of the carbonyl peaks.

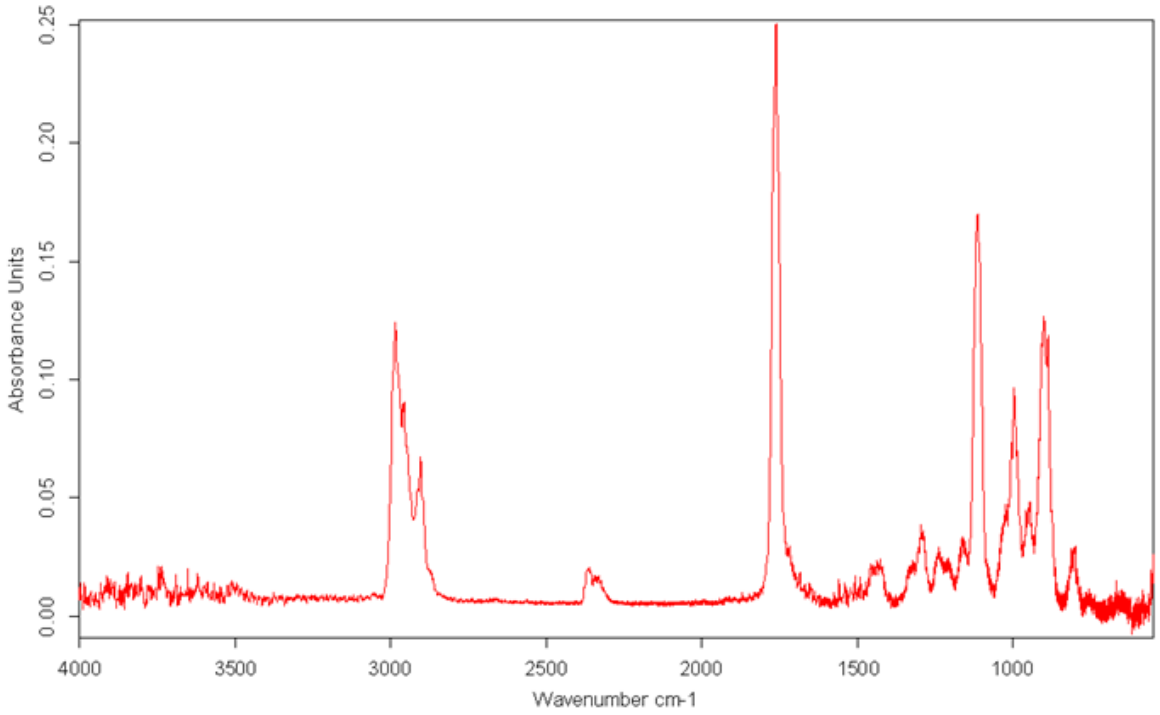

Figure 2.6 Gas phase IR spectrum of neat Cyrene.

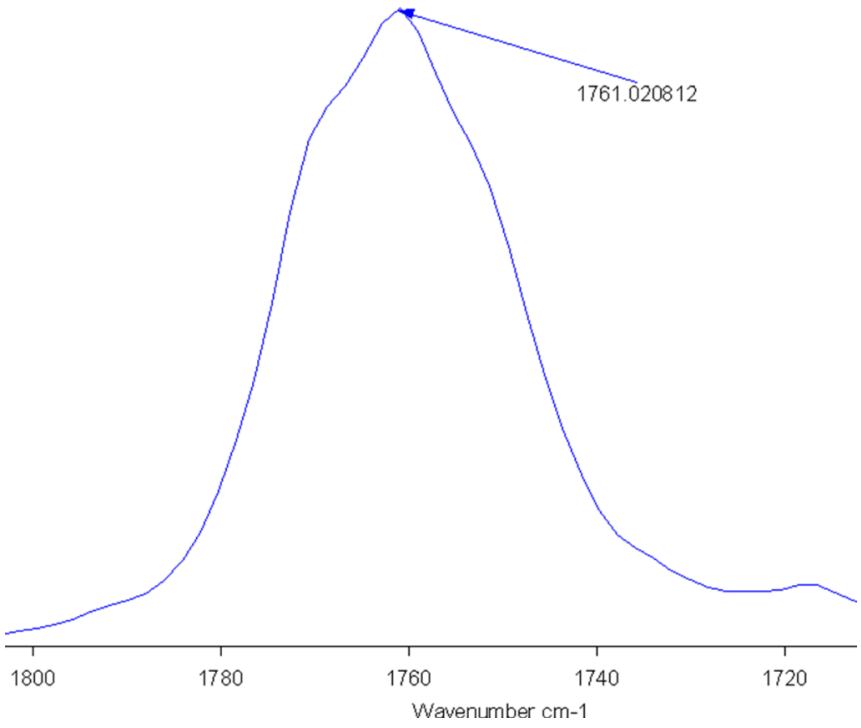

Figure 2.7 Close-up of the carbonyl region in the gas phase IR spectrum.

Possible explanations to this phenomenon could be the existence of strong hydrogen bonding or just a very diffuse hydrogen bonding between the Cyrene molecules.

Judging the structure of Cyrene, the only possible intermolecular hydrogen bonding is between the oxygen of the carbonyl group and the bridge proton next to it, as the latter is the most 'acidic'. Such an interaction would represent a bond strength between -1,9 and -5,5 KJ/mol[67,68] which is weak yet significant enough to stabilize oligomers.

2.1.3 Fermi resonance or not?

As previously discussed the spectroscopic splitting of an IR band can be attributed to a wide range of causes, one of which was the potential occurrence of Fermi resonance. In order to prove or disprove this theory, the spectroscopic behaviour of Cyrene in different solvents was investigated. It was found that in water and D_2O the band at 1725 cm^{-1} widens and increases in intensity and the band at 1743 cm^{-1} decrease. In toluene the intensity of the carbonyl band is reduced (Figures 2.8-2.9). Here the most intense band at about 1743 cm^{-1} decreases in intensity in the polar solvents and shows a slight blue shift of just 1-2 cm^{-1} (1745 cm^{-1}).

The observed behaviour of the carbonyl group bands in the presence of polar/apolar solvents is contrary to the expectation in that the free carbonyl group,[52,69] i.e. the carbonyl band should show a strongest shift.

Alternatively this strange behaviour could potentially be explained by the occurrence of Fermi resonance.[70] In general, Fermi resonance results in the splitting of two vibrational bands that have nearly the same energy and symmetry in both IR and Raman spectroscopies. The two interacting bands are usually a fundamental vibration and an overtone or combination band.[71] As a consequence of their interaction one does not observe the expected strong band for the fundamental and the weak band for the overtone or combination band but rather two intense bands in the IR spectrum.[72] If two vibrational mode have the same symmetry and similar energies, mixing occurs and the resulting modes can be described by a linear combination of the two interacting modes.[73] The effect of this interaction is a split between their energy levels, and consequently also an increase in the distance between the peaks.[74] The mixing of the two states also tends to equalize the intensities of the bands involved in the Fermi resonance, and a weak overtone or combination band shows significant intensity while the fundamental band tends to decrease its intensity. Because the coupling bands are close in frequency, the interaction could be affected if one band undergoes a frequency shift, for instance due to deuteration or the presence of a solvent, while the other does not. This shift in the vibration frequency leads to decoupling of the two bands.[24,2575,76] It is also noteworthy that the relative intensities of the components of a Fermi resonance multiplet can vary significantly with the temperature if the frequency of one of the resonant bands changes (e.g. the C=O fundamental).[77,78]

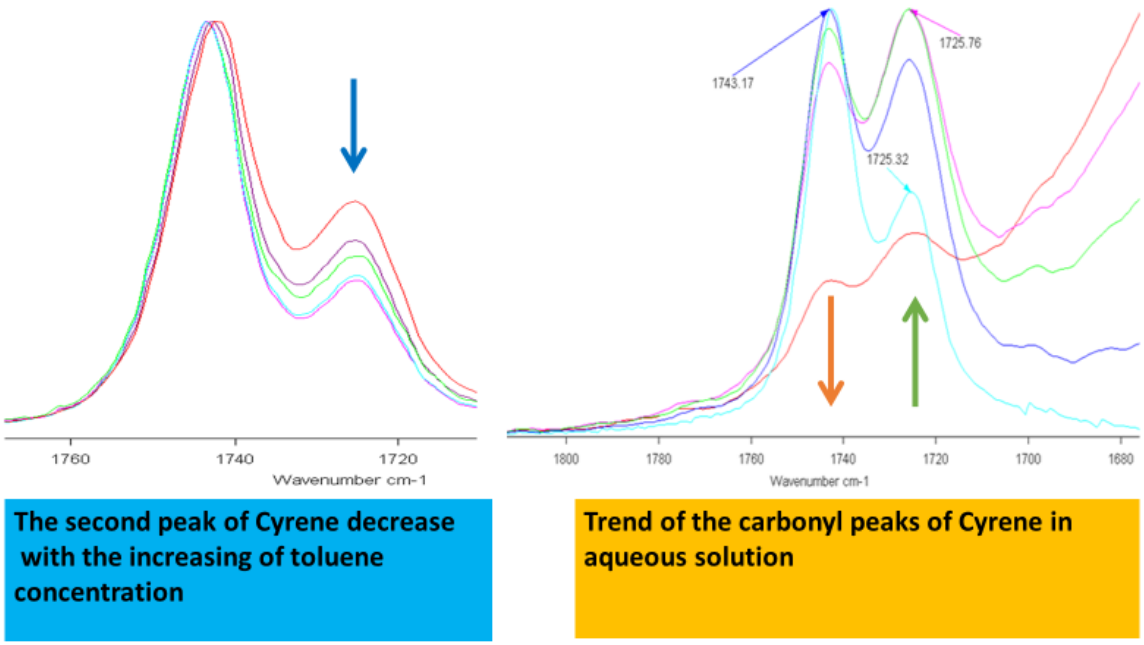

Figure 2.8 Evolution of the carbonyl IR peaks with increasing amounts of toluene and H_2O.

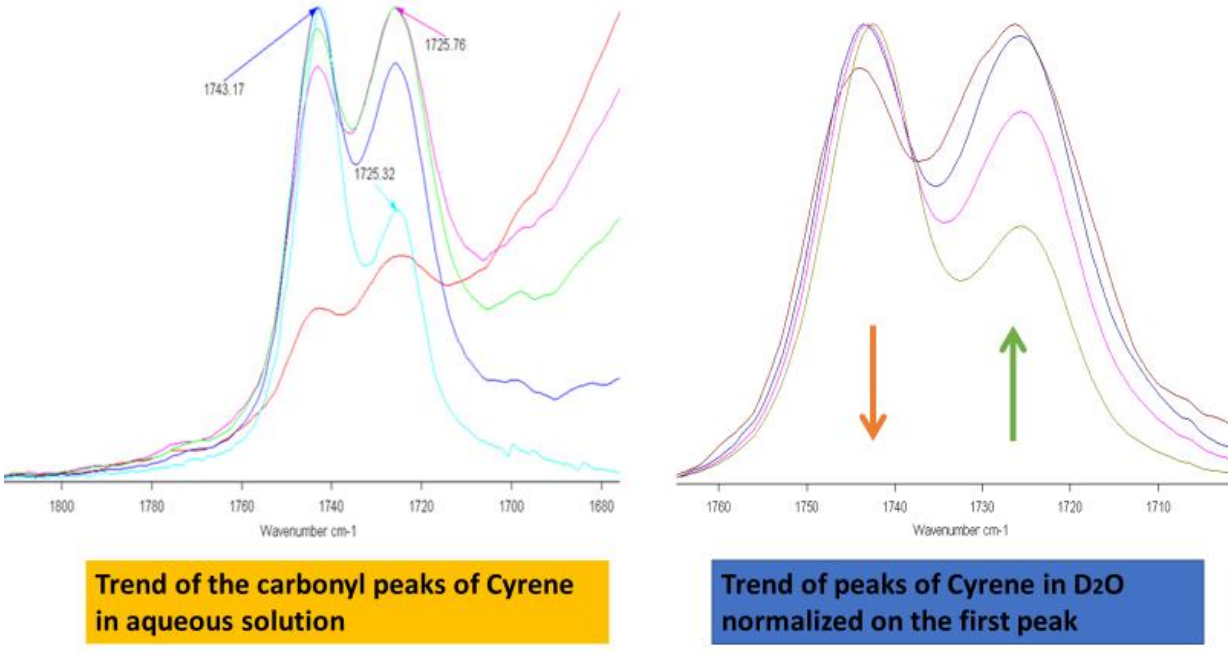

Figure 2.9 Evolution of the carbonyl peaks with increasing amounts of H_2O and D_2O.

As was shown above the IR spectra of Cyrene do not demonstrate conventional characteristics for a carbonyl (See Figure 2.5 and Figures 2.8-2.9). This behaviour could be indicative of a very diffuse hydrogen bonding between the Cyrene molecules. In the case of two different conformers, an increase in the temperature should result in an increased difference in the relative intensity of the bands with then also a corresponding sizeable change in the shape of the bands in the fingerprint region.[79,80,81] However, this was not observed in the IR spectra of both gas and condensate phase.

In order to prove/disprove the possible presence of a Fermi resonance many methods can be used. These include the "solvent variation method" which is a semi-empirical method valid for a large range of molecules.[59] Through this method one can obtain/calculate the value of the Fermi constant coupling. A constant value of the Fermi constant over a range of solvents provides strong evidence for the occurrence of Fermi resonance.[59] To calculate this constant one needs of data:

1) the ratio between the intensity of the two peaks in the carbonyl region in different solvents and 2) knowledge on the distance between the maximum intensity of the peaks, also for different solvents.[59] The coupling constant can then be calculated using the following equation (Equation 2.3):

$$R= \{\Delta +(\Delta^2-4W^2)^{1/2}\}/\{\Delta- (\Delta^2-4W^2)^{1/2}\} \qquad \text{[Eq.2.3]}$$

Were R is the ratio between the integrated intensity of peaks, W is the Fermi resonance coupling constant and Δ is the difference in frequency between the peaks at maximum intensity.

Another test to prove or disprove Fermi resonance reported in literature is the effect isotopic substitution has on Fermi resonance. As an additional benefit this technique could also rule out the possible existence of two different molecular conformations – which could also be the reason for the double carbonyl group observation in IR spectroscopy.[58,82,83] Applied to Cyrene this would require isotopic labelling with deuterium alpha to the carbonyl group (either side). As this was considered unpratical and also very expensive, as such this route was not further pursued.

Cyclopentanone is a literature example of a Fermi resonance which presents a double carbonyl group in its IR spectrum.[84,85,86] However, as cyclopentanone does not show the characteristically expected Fermi resonance behaviour when applying the solvent variation method, some doubt exists and it was also suggested by the authors that the appearance of a double carbonyl group could equally be due to the presence of a dimer.[59,84-87] By application of the same methodology described by these authors it was hoped that Fermi resonance could be proved or disproved. More specifically the intensities of the two observed carbonyl peaks should not change between the Raman spectra recorded with and without polarized infrared light. The non-polarized and polarized Raman spectra for pure Cyrene (at room temperature) are shown in Figures 2.10 and 2.11. It can be seen from these figures that the relative intensities of the two carbonyl peaks do change to a certain degree.[85,86] It can thus be said that it is unlikely that Fermi resonance is at the origin of the double carbonyl group observed in the IR spectrum of liquid Cyrene.

Additionally the use of a state-of-the-art React-IR instrument was tried to get potentially a better view on the influence of temperature on the IR spectra of Cyrene. (Figure 2.12-2.13) Unfortunately, the resolution of the React-IR's was only 4 cm^{-1}, the differentiation between the two apparent carbonyl bands was found to be limited.

Nonetheless using this technique little real change can be seen of the overall shape of the combined carbonyl peaks with the temperature in the 25-130 ^{o}C range.

Although the experimental data obtained within this thesis is against the occurrence of Fermi resonance, the only method that can excluded with certainty is the use of isotopic substitution.

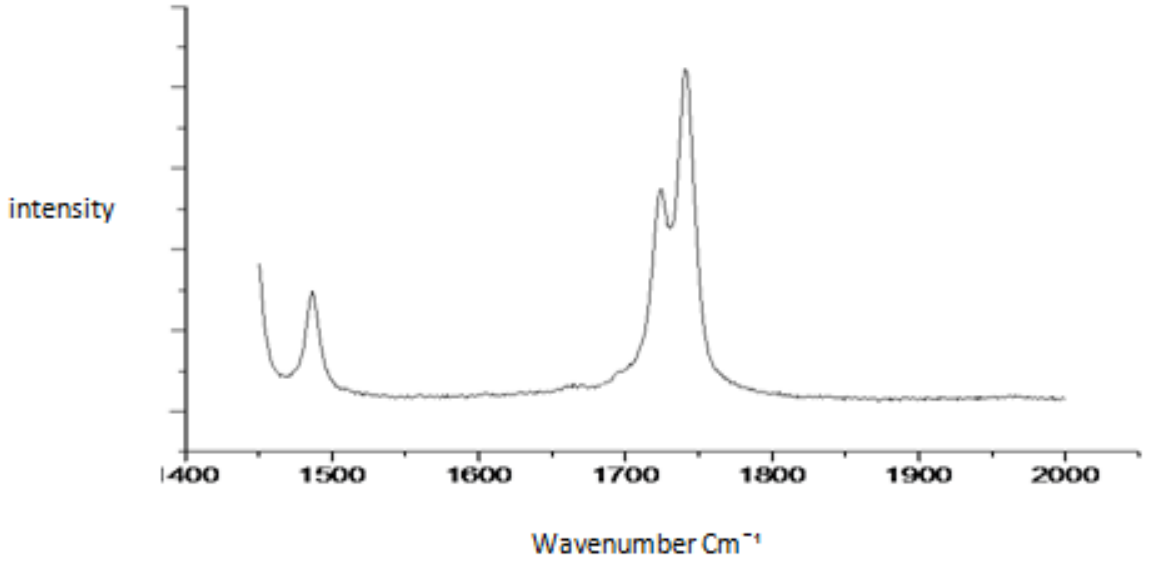

Figure 2.10 Non-polarized (normal) Raman spectrum of neat liquid Cyrene.

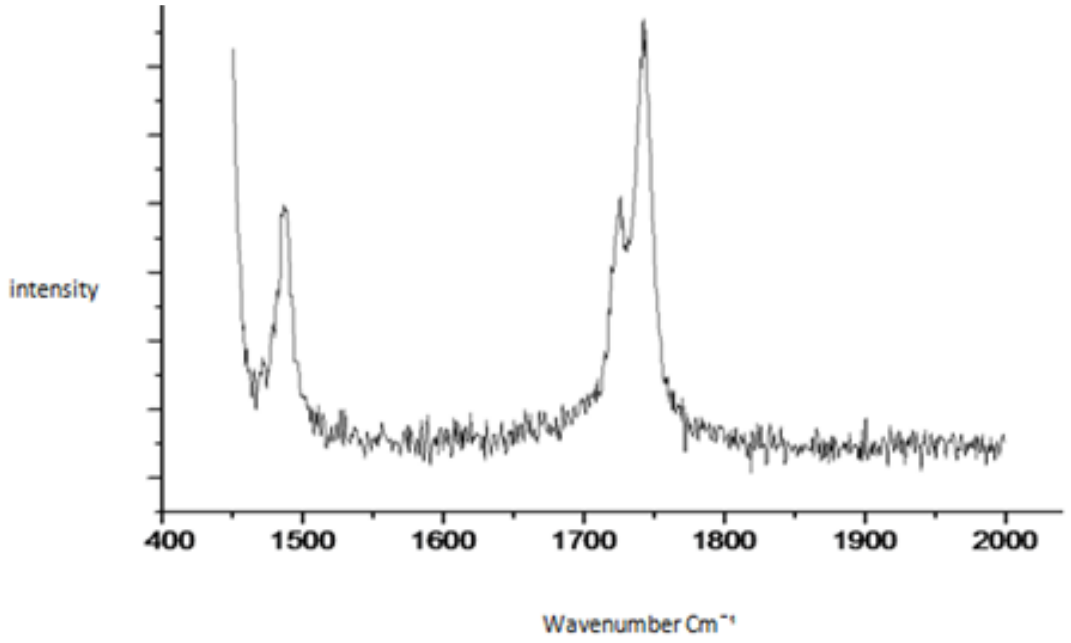

Figure 2.11 Polarized Raman spectrum of neat liquid Cyrene.

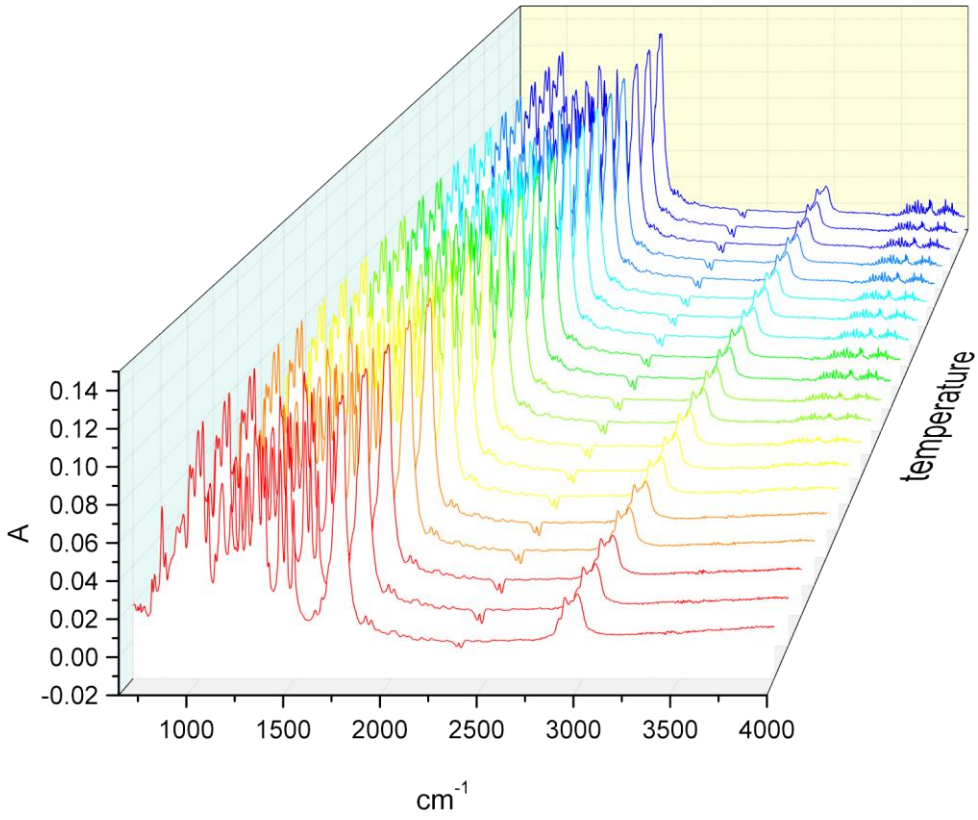

Figure 2.12 React IR spectra of neat liquid Cyrene recorded between 25-130 °C.

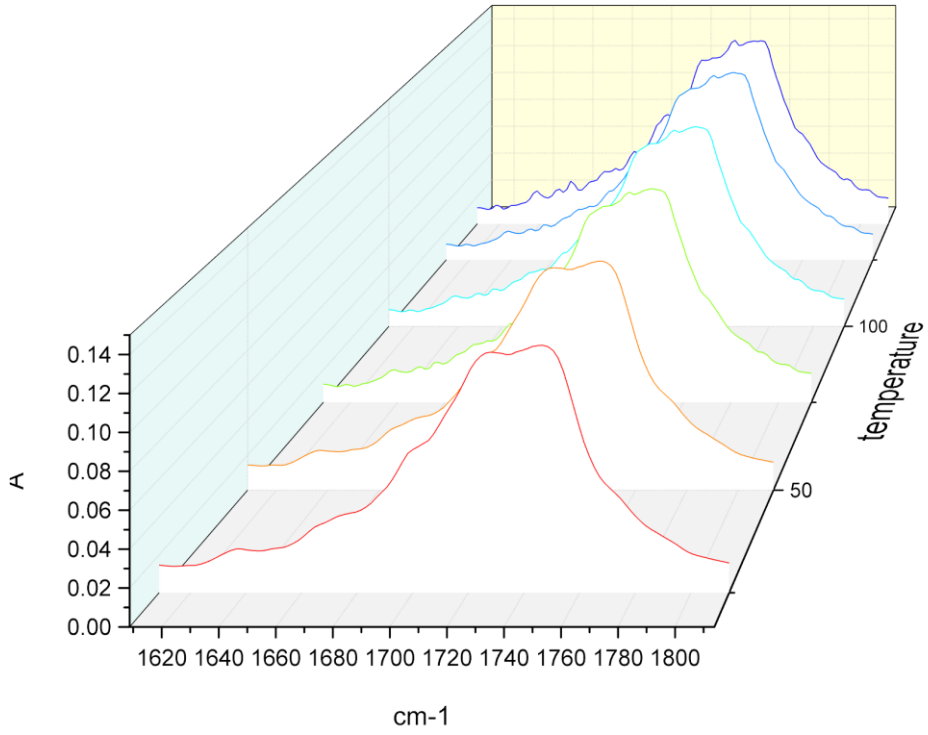

Figure 2.13 Close-up on the carbonyl region of the temperature React-IR spectra displayed in Figure 2.12

2.1.4 Potential oligomerization of Cyrene

In this section the experimental data gathered on Cyrene is resampled to test for the existence of a possible degree of organization in neat liquid Cyrene. As in the above section (2.1.3) it has been shown that Fermi resonance is unlikely the reason for the occurrence of a double carbonyl group in Cyrene's IR spectrum, the question to its cause remains thus open. One other option is intermolecular hydrogen bonding, and thus oligomerization, potentially even taking the form of some more defined structural organization. From the Kamlet–Abboud–Taft parameters of Cyrene (Table 1.2) it could be derived that this solvent is aprotic, the value of π* value (corresponding to dipolarity) being close to those of highly dipolar aprotic solvents. It should however be noted that the β value is slightly lower than would have been expected for dipolar aprotic solvents. This is important as it does indicate for some hydrogen bond accepting capability.[88] As such the existence of some intermolecular hydrogen bonding between Cyrene molecules is thus not an absolute impossibility, and can be verified calculating the ΔH and ΔS of vaporization of pure Cyrene at boiling point. The former can be determined through the classic Clausius-Clapeyron equation (equation 2.4). As can be seen from Figure 2.14, plotting Ln(P) (Y-axis) to 1/T (X-axis) (see again equation 2.4) yields a straight line, the slope being equal to $-\Delta H_{vap}/R$ (equation 2.5). The so calculated enthalpy of vaporization of pure Cyrene is 67.142 KJ/mol. This value is substantially larger than the one calculated using ACD/labs yielding a ΔH_{vap}=46.83 ±3 KJ/mol at boiling point. (See Figure 2.15.)

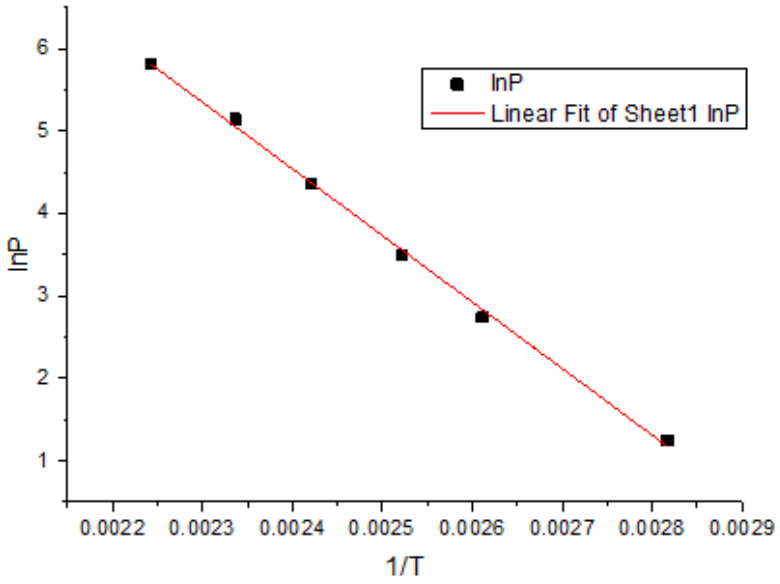

Figure 2.14 Ln(P) plotted as a function of 1/T (T being expressed in Kelvin) – evaluating the Clausius- Clapeyron equation.

$$ln\left(\frac{P_1}{P_2}\right) = \frac{\Delta H_{vap}}{R}\left(\frac{1}{T_2} - \frac{1}{T_1}\right) \qquad \text{[Eq.2.4]}$$

$$Slope = -\frac{\Delta H_{vap}}{R} \qquad \text{[Eq.2.5]}$$

Compound structure

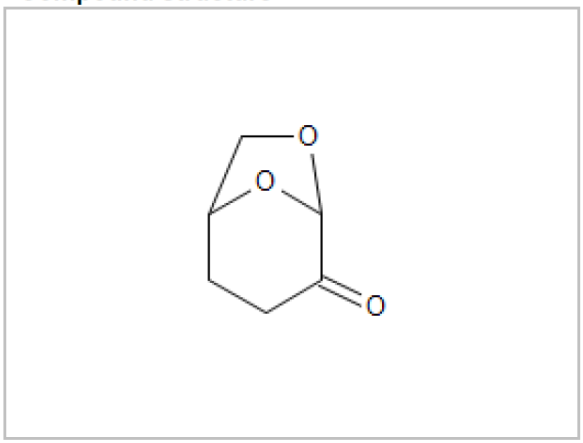

Boiling Point:
BP (deg C at 760.00 mmHg) = 231.64 +- 30.00

Vapor Pressure:
$\log_{10}(p)$ = -1.210 +- 0.46 (p in mmHg)
p (at 25.00 deg C) = 0.0617 mmHg

Enthalpy of Vaporization:
$\text{delta}_{vap}H(T_{boiling\ point})$ = 46.83 +- 3.0 *kJ/mol*

Figure 2.15 Theoretical calculation of the enthalpy of vaporization by the ACD/Labs software.

Knowledge of ΔH_{vap} allowed for the calculation of the entropy of vaporization ΔS_{vap} using equation 2.6.

$$\Delta S_{vap} = \frac{\Delta H_{vap}}{T} \qquad \text{[Eq.2.6]}$$

This yielded a ΔS_{vap} of 137 J/mol K. This is substantially higher than the constant value of 85–88 J/mol K, commonly known as Trouton's rule. Exceptions to this rule are the entropies of vaporization of water, ethanol, formic acid and XeF_6 – the latter being 136.9 J/mol K which is actually very similar to the one obtained for Cyrene. The positive deviation is due to the existence of special interactions (e.g. hydrogen bonding) between the individual molecules in these liquids.[38-41] [89-92]

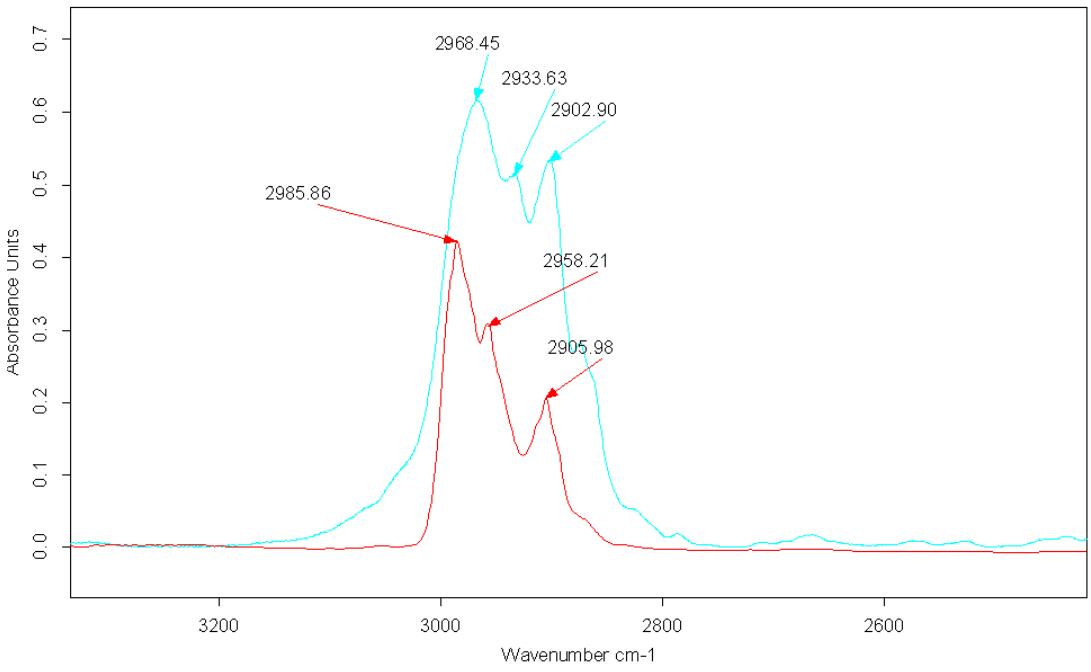

Figure 2.16 C-H stretching zones of the IR spectra of liquid (blue) and gas phase (red) IR spectra of Cyrene.

The existence of hydrogen bonding can also be inferred from the C-H stretching zone of both the liquid and gas IR spectra (Figure 2.16). In going from the gas to the condensed phase, most of the C-H in Cyrene display clear red shifts: 2985 $\rightarrow$ 2968 cm^{-1} and 2958 $\rightarrow$ 2933 cm^{-1}. This is consistent with lengthening of X-H bonds in the presence of an atom Y having lone pair electrons such as oxygen.[93] In Cyrene oxygen can be found in the carbonyl group but also in the acetal group – all of these oxygens can effectively be involved in hydrogen bonding. The limited shift from 2905 $\rightarrow$ 2902 cm^{-1} points at the presence of a less polar, electron poor X-H bond, the best candidate being the bridghead proton alpha to the carbonyl group (calculations do reveal some acidity at this position).[93]

In a further advancement FT-IR spectroscopy of Cyrene in very dilute solution with CCl_4 (Cyrene:CCl_4 molar ratio of 1:200) was performed (Figure 2.17). Interestingly, using these conditions (high dilution in CCl_4) only one carbonyl group band at 1749 cm^{-1} could be observed in the IR spectrum. This is further proof for intermolecular aggregation in liquid Cyrene, the presence of CCl_4 and the high dilution favouring monomeric Cyrene and thus the appearance of only one carbonyl group stretch in the IR spectrum.[4394]

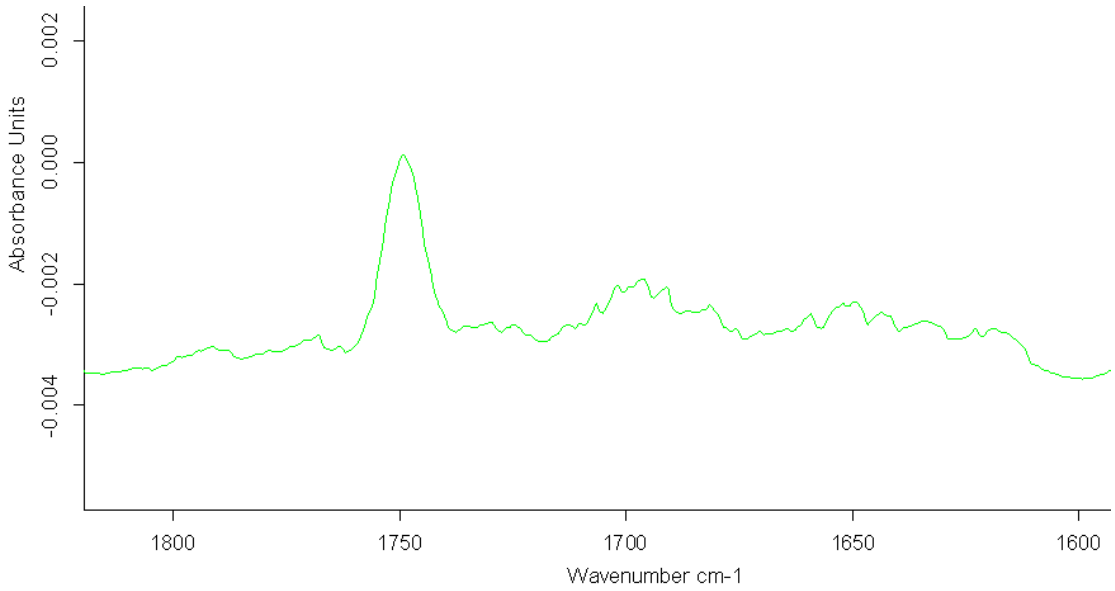

Figure 2.17 IR spectrum of highly diluted Cyrene in CCL_4 (1 to 200 ratio by mol).

To gain still more understanding calculations of the gas phase IR spectra of monomeric Cyrene (Figure 2.18) and a Cyrene dimer (Figure 2.20) were performed by Dr. Martin Cockett. The similarity of the calculated gas phase IR spectrum of monomeric Cyrene with the experimentally obtained gas phase IR spectrum (see Figure 2.6) is apparent holding also in the finger print region. While the gas phase IR spectrum of monomeric Cyrene shows only one carbonyl group, the gas phase IR simulation of the Cyrene dimer (dimer shown in Figure 2.19) did effectively reveal the presence of two distinct carbonyl stretches (Figure 2.20). Note however that this dimer is not equal to the one tentatively depicted in Figure 2.4 in which the dimerization involves the double interaction between the carbonyl groups and the bridgehead C-H groups alpha to these. For such a dimer the calculated gas phase IR spectrum reveals only one carbonyl group stretch.

As the dimer shown in Figure 2.19 is configured it is clear that two different chemical environments arise for the two involved carbonyl groups. This is appreciable proof for the existence of intermolecular hydrogen bonding in liquid Cyrene. Evidently it is possible that the reality in liquid Cyrene does not concern the existence of true dimers but rather trimers or (undefined) oligomers or combinations of all these. Currently more elaborate calculations are being performed to shed more light on this.

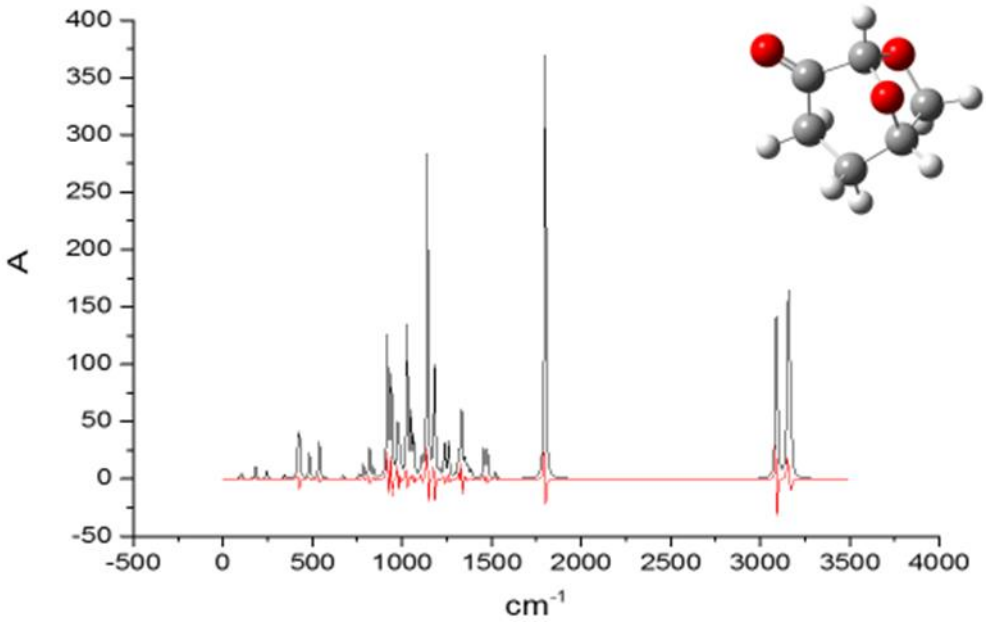

Figure 2.18 Shows the calculate IR spectra for monomeric Cyrene.

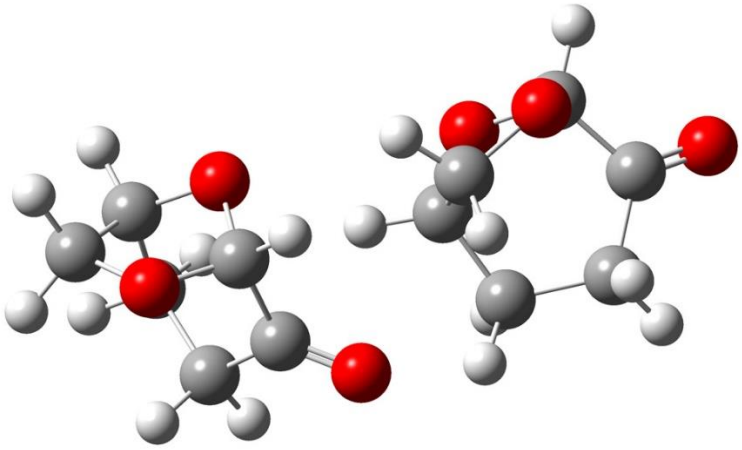

Figure 2.19 Dimer used for the calculation of the IR spectrum shown in figure 2.20.

The likely existence of dimerization/oligomerization in liquid Cyrene, brings up the question of whether any long range order exists in liquid Cyrene. For this reasons liquid Cyrene was also investigated using a polarized optical microscopy and diffuse light scattering. The existence of a strong dipole in Cyrene, shown in Figure 2.21, 3.4 Debye in nominal value and passing through the plane between the carbonyl and the alpha bridgehead carbon to it, combined with its ability to self-associate (likely intermolecular hydrogen bonding between Cyrene molecules) could well impart

some kind of liquid crystalline behaviour. Also the (weak) amphiphilicity in Cyrene could still account for the formation of micelles, which are detectable with diffuse light scattering. Liquid crystalline behaviour could not be established and DLS was inconclusive.

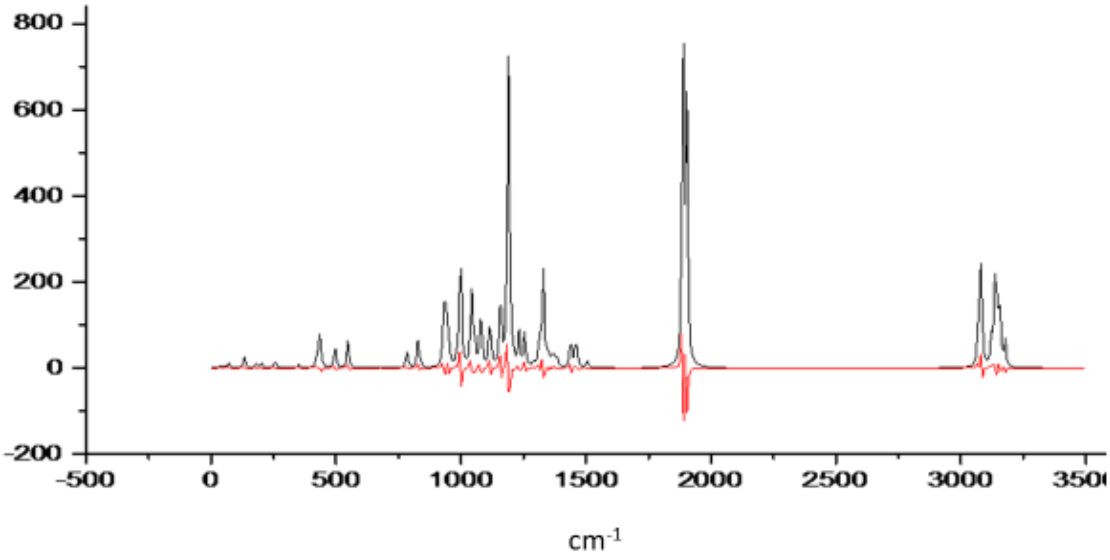

Figure 2.20 Calculated gas phase IR spectrum of the Cyrene dimer shown in Figure 2.19.

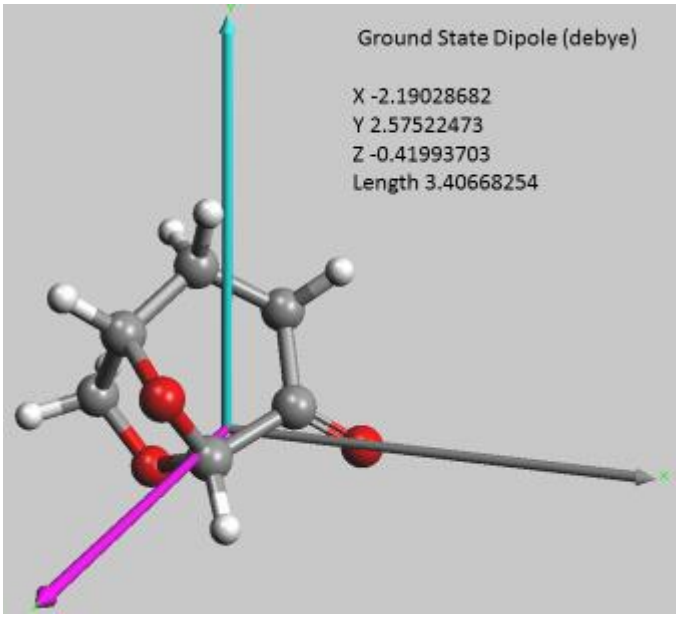

Figure 2.21 Calculation of the dipole vector of Cyrene.

Complementary to the polarized light microscopy and diffuse light scattering work, Cyrene was also subjected to differential scanning calorimetry (DSC) allowing gathering of valuable information on its crystallization and melting. Figure 2.22 shows the last heating cycle from which it is in principle possible to assess any amorphous behaviour of pure Cyrene. While a glass transition temperature could not be identified (-70 °C being the lowest working temperature of the DSC instrument), an exothermic peak at -64,5 °C, likely related to cold crystallization of Cyrene, could be clearly

identified. Cold crystallization is an exothermic process which is observed on heating a sample that has previously been cooled very fast and has had no time to crystallise.[95] It was found possible to avoid cold crystallization using the following method:

- equilibrate -70 °C
- modulate+/- 1 °C every 60 s
- isothermal for 5 min
- ramp 2 °C/min to 50 °C

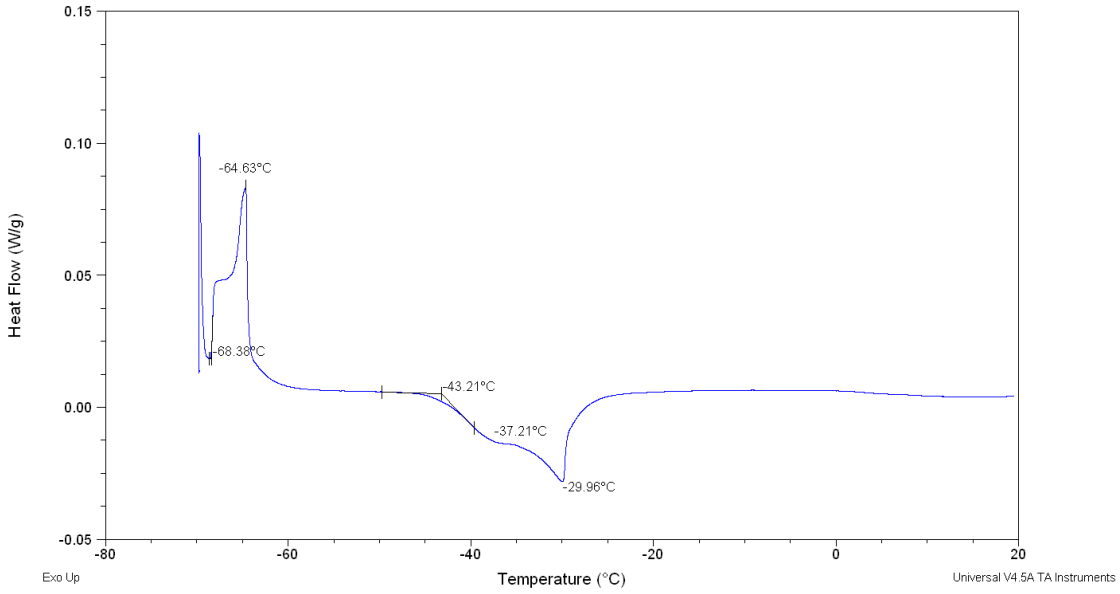

Figure 2.22 DSC heating curve thermograph of liquid Cyrene.

Figure 2.23 shows the heating curve of the DSC run using the above method and does indeed not show a cold crystallization peak. Note however the appearance of two peaks for the melting point. The relative ratio of these was found quite dependent on a) the history of the Cyrene sample, changing markedly when RT Cyrene is used compared to Cyrene stored in a fridge and b) the heating & cooling rates. No glass transition temperature could be observed. The observation of two melting peaks points at the existence of two crystal types and thus polymorphism. No thermal peak corresponding to the presence of a liquid crystalline phase could be found. This absence of long range order shows also from SAXS measurements which will be discussed in Chapter 3.

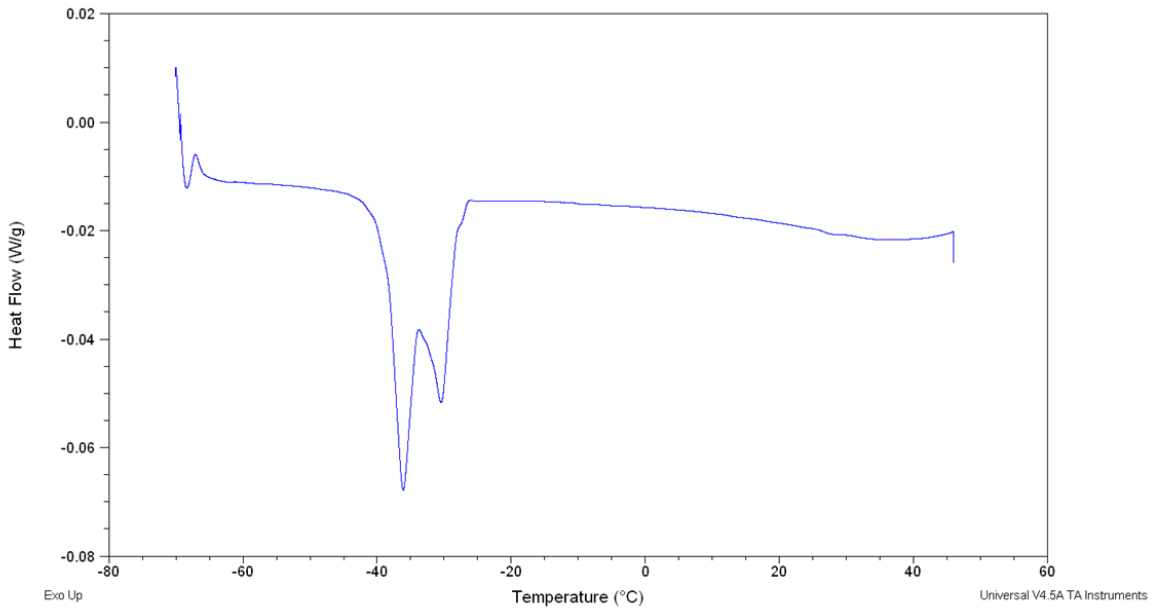

Figure 2.23 DSC thermograph of liquid Cyrene run using a method avoiding cold crystallization (heating curve only).

Chapter 3: *Interaction of Cyrene with water*

Chapter 3

3.1 The hydrates/geminal diols of carbonyl groups: a brief overview

Cyrene contains a carbonyl functional group. In the presence of water, aldehydes and ketones tend to be in equilibrium with their hydrate (also known as 'geminal diol'). The equilibrium position in this type of reaction is influenced by both steric hindrance and the electronic effects of substituent groups close to the carbonyl group. With the majority of ketones the equilibrium position lays on the ketone side of the equilibrium, but with aldehydes the presence of the geminal diol can be more dominant.

The case of acetaldehyde is exemplary: the stability of its hydrate form finds its origin in a weaker π component of its carbonyl group than compared with other aldehydes or ketones. Also the small steric hindrance of the hydrogen atoms plays an important role here. For ketones the situation is generally different, for instance, in the case of acetone the carbonyl group is actually stabilized by the methyl groups, them being electron donating and thus stabilizing the partial positive charge of the carbon of the carbonyl group. Evidently steric hindrance has a negative effect on the formation of a geminal diol. The case of cyclic ketones, as is Cyrene, is still different as for instance cyclopropanone in water does exist solely as its hydrate. The driving force here is a release of internal strain.[96] The equilbrium reaction between Cyrene and water is depicted in Figure 3.1.

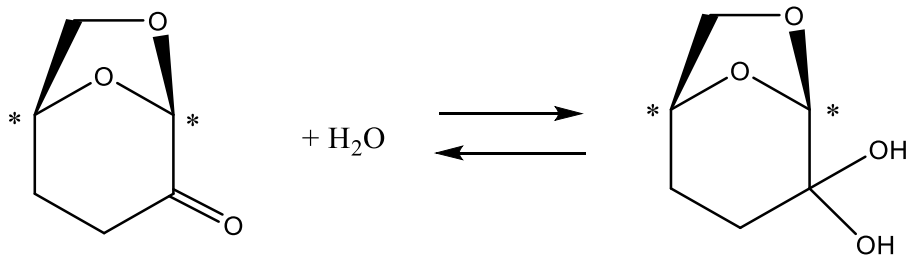

Figure 3.1 The ketone/hydrate equilibrium of Cyrene in the presence of water.

It is often impossible to isolate, physically, the geminal diol as the removal of water will reform the ketone. An exception to this rule is the hydrate of trichloroacetaldehyde due to a strong stabilization effect caused by the interaction between the hydrogens of the diol and the Cl atoms.[97] In the case of Cyrene we have not been able to isolate the geminal diol.

3.2 Infrared spectroscopy applied to the cyrene/geminal diol equilibrium

In order to describe the behaviour of the Cyrene/geminal diol/H_2O (or D_2O) ternary mixture a wide range of spectroscopic experiments were performed. A series of FT-IR spectra of Cyrene dissolved in water and D_2O at different dilution were collected (Figure 3.2 and Figure 3.3).

From Figure 3.2 it can be clearly seen that the first carbonyl peak at 1743 cm^{-1} decreases with increasing H_2O content while the second carbonyl peak at 1725 cm^{-1} is less affected. The second

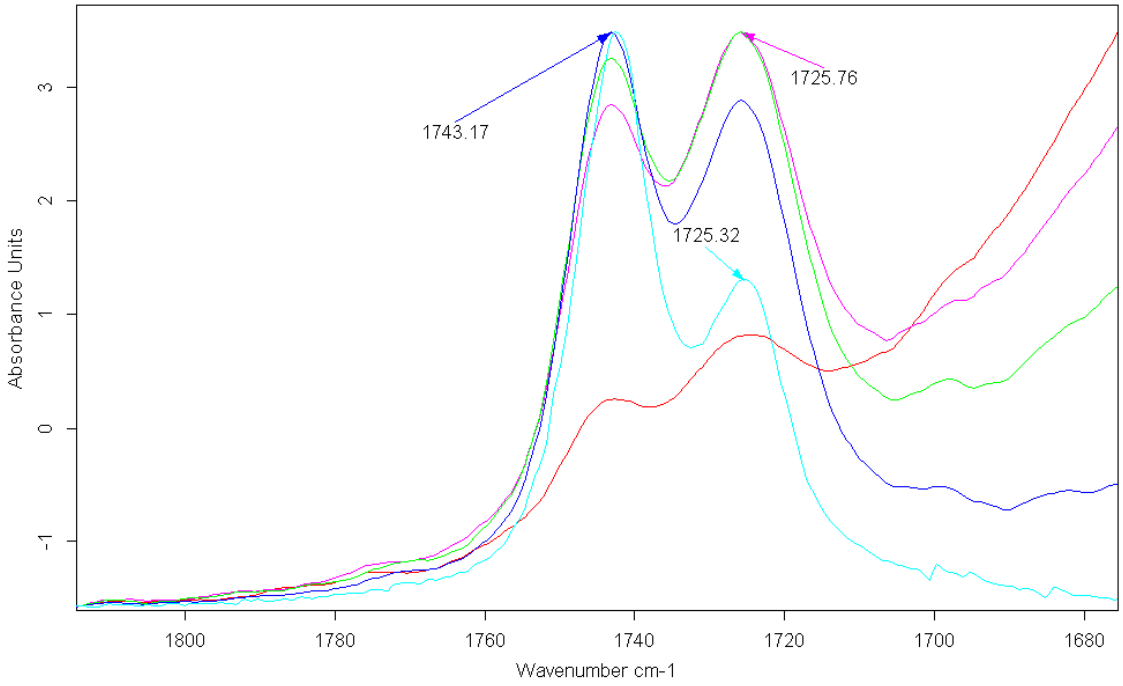

Figure 3.2 Evolution of the carbonyl group stretch in FT-IR with increasing presence of H_2O: *in light blue* Cyrene 100%, *in blue* Cyrene 80%, *in green* Cyrene 70%, *in purple* Cyrene 65%, *in red* Cyrene 50%.

carbonyl peak seems to widen which can point at hydrogen bonding between water and the Cyrene molecule. In depth investigation of the Cyrene/ H_2O /geminal diol equilibrium was found impossible due to the complexity of the system but also while the relevant IR bands of the geminal diol situate themselves in the fingerprint region, overlapping with other peaks. Additionally in excess of water (> 50 wt%) the water peak ~ 1650 cm^{-1} (δ_{H2O} bending mode) started largely interfering with the carbonyl region.

FT-IR spectra of the Cyrene/D_2O/geminal diol ternary mixture is more revealing limiting the interference in the carbonyl region (Figure 3.3). Normalizing on the peak at higher wavenumber (1743 cm^{-1}) one can clearly see a relative increase of the second carbonyl peak (1725 cm^{-1}) with increasing water content.

This odd behaviour basically attributes a certain resistance of the carbonyl group appearing at the lower wavenumber (1725 cm^{-1}) towards reaction with water. This is consistent with the previous

finding in Chapter 2 where through calculation liquid Cyrene was found/confirmed to have a certain degree of molecular ordering (dimerization – oligomerization) clearly identifying the presence of two different types of carbonyl groups.

FT-IR spectroscopy was found unsuitable to determine the composition of the Cyrene/geminal diol/H_2O (or D_2O) ternary mixtures. This could instead be achieved by using $^{1}H/^{13}C$ NMR spectroscopy which will be discussed later.

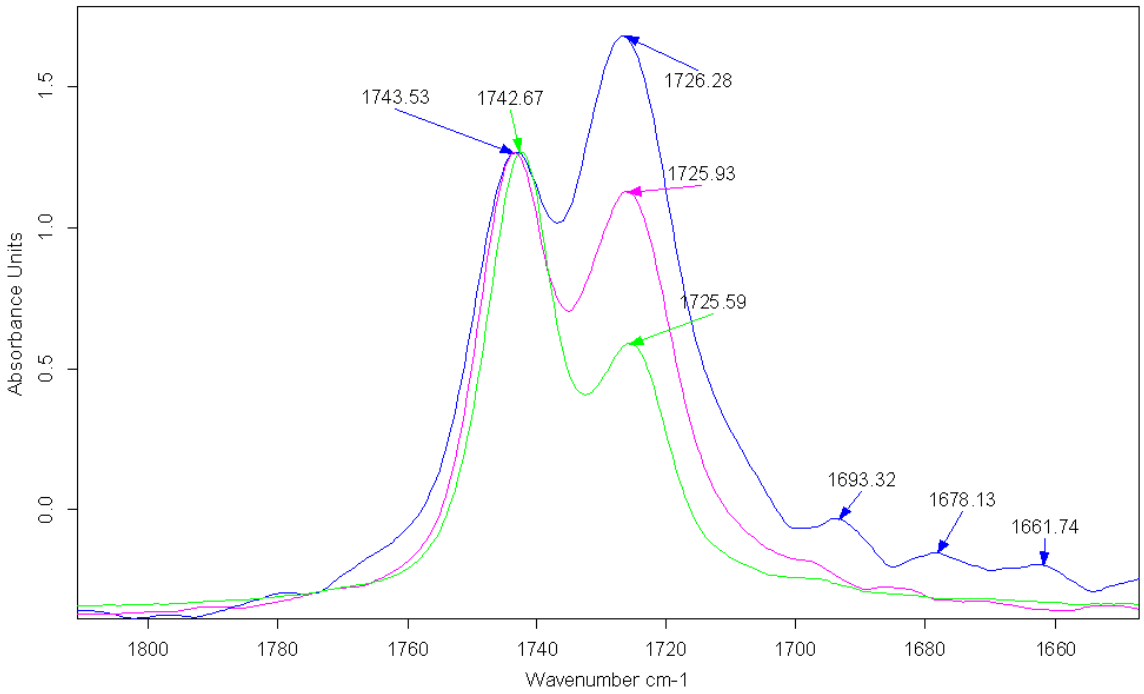

Figure 3.3. Evolution of the carbonyl group stretch in FT-IR with increasing presence of D_2O*: in green Cyrene 100 wt%, in purple* 75 wt% Cyrene*, in blue* Cyrene 55 wt%. All the spectra were normalised on the 1742 cm^{-1} peak.

3.3 Differential scanning calorimetry (DSC) applied to the cyrene/geminal diol equilibrium

The physical behaviour of the Cyrene/geminal diol/H_2O ternary mixture changes drastically with the temperature. All below reported DSC data was obtained using the following temperature programming: for all the DSC data reported was used the following method:

1) equilibration at 20°C,
2) cooling at 5°C/min to -70°C,
3) heating at 15°C/min to 20°C (x 2 times)

The method above was found particularly useful for Cyrene/water compositions up to about 45 wt% Cyrene, keeping also the effect of water super cooling under control. Some examples of DSC thermograms obtained for initial Cyrene concentrations lower than 50 wt% (in water) are shown in

Figures 3.4. It was possible to derive the melting points for various combinations of Cyrene and water from the DSC thermograms using the onset function available in instrument's software, as is shown in Figure 3.5. The DSC derived melting points were compared to the ones obtained by a fibre optic probe – the Cyrene/geminal diol/water ternary mixtures being frozen using liquid nitrogen. Figure 3.6 shows the melting and freezing points determined by DSC and fibre optic probe.

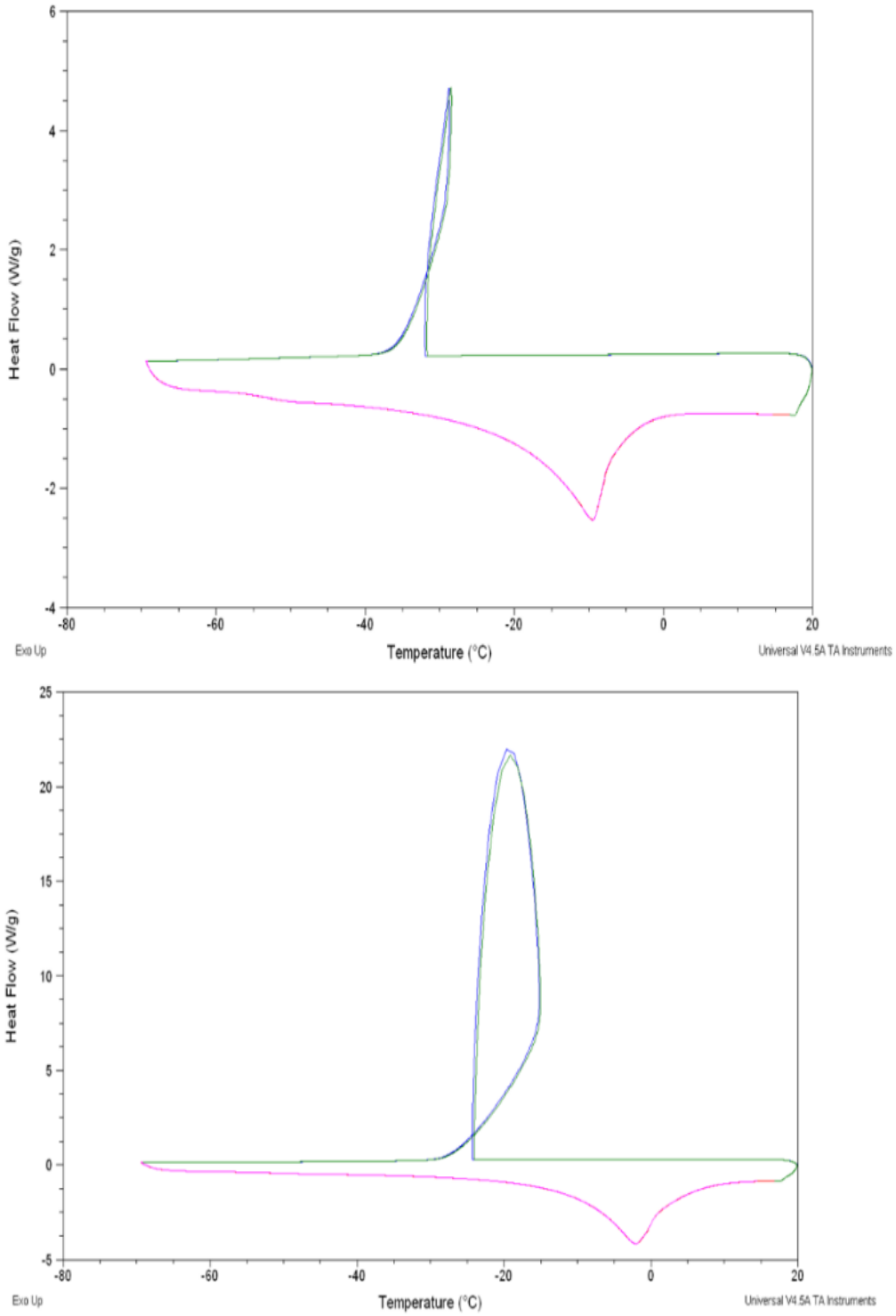

Figure 3.4 A Some examples of DSC thermograms obtained for Cyrene/water compositions lower than 50 wt% Cyrene.

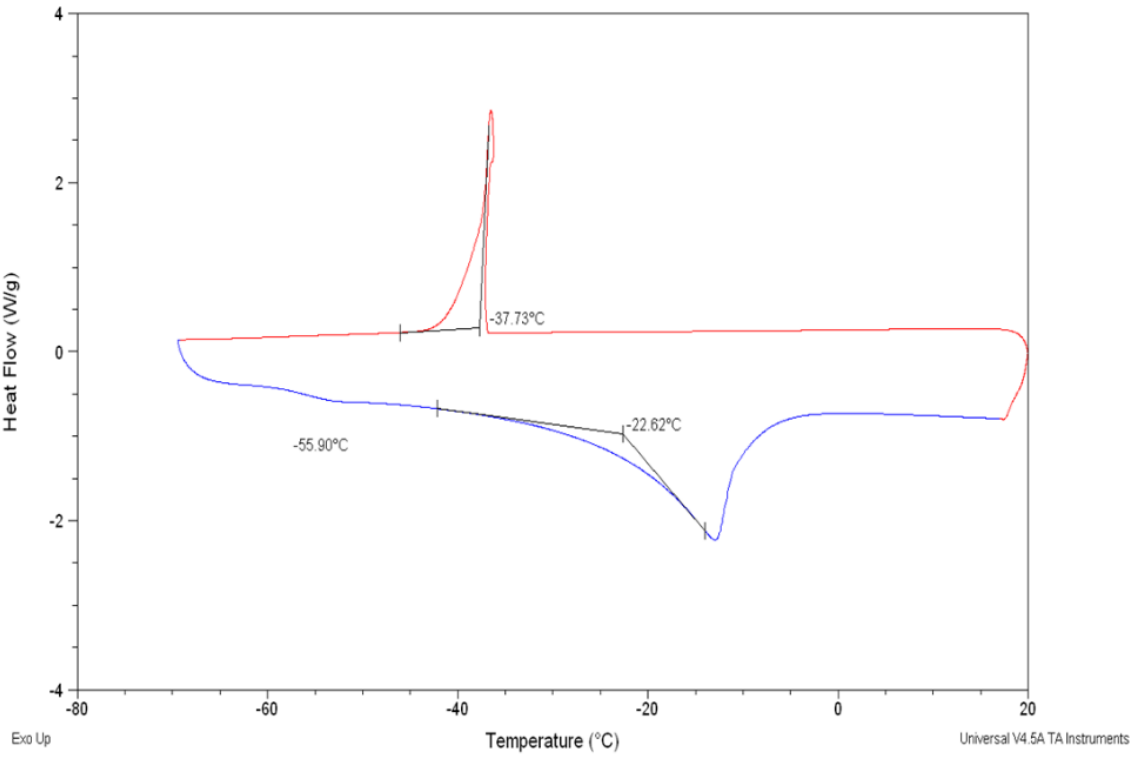

Figure 3.4 B Some examples of DSC thermograms obtained for Cyrene/water compositions lower than 50 wt% Cyrene.

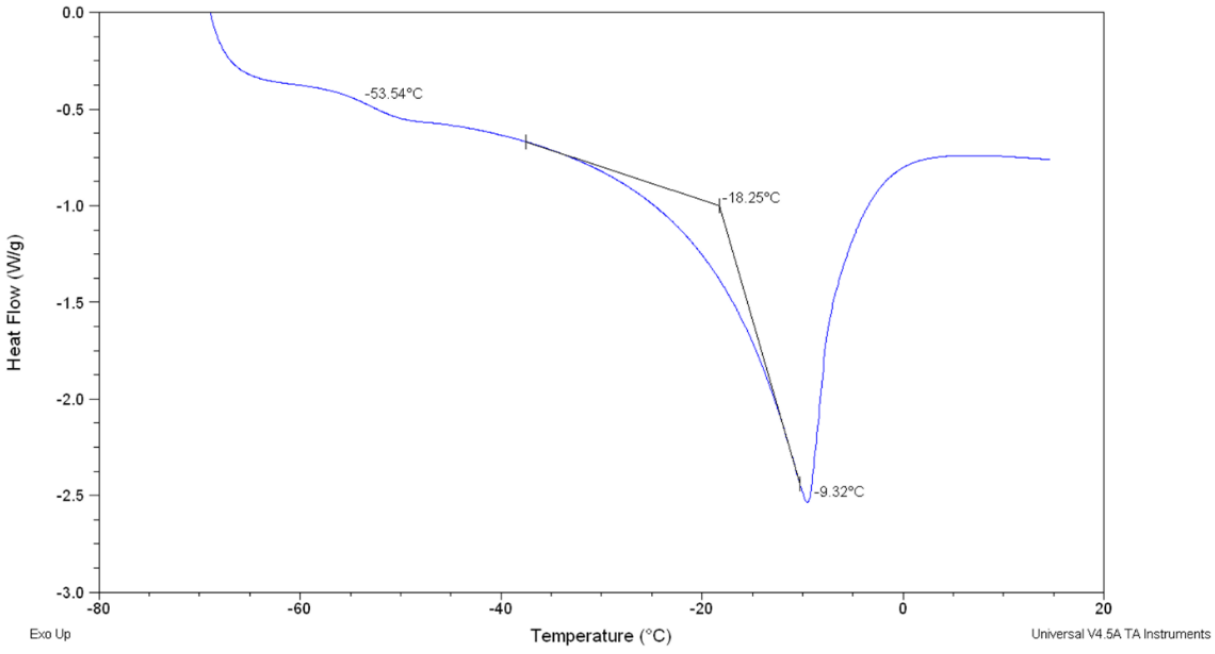

Figure 3.5 Example of a melting point calculation in DSC using experimental onset.

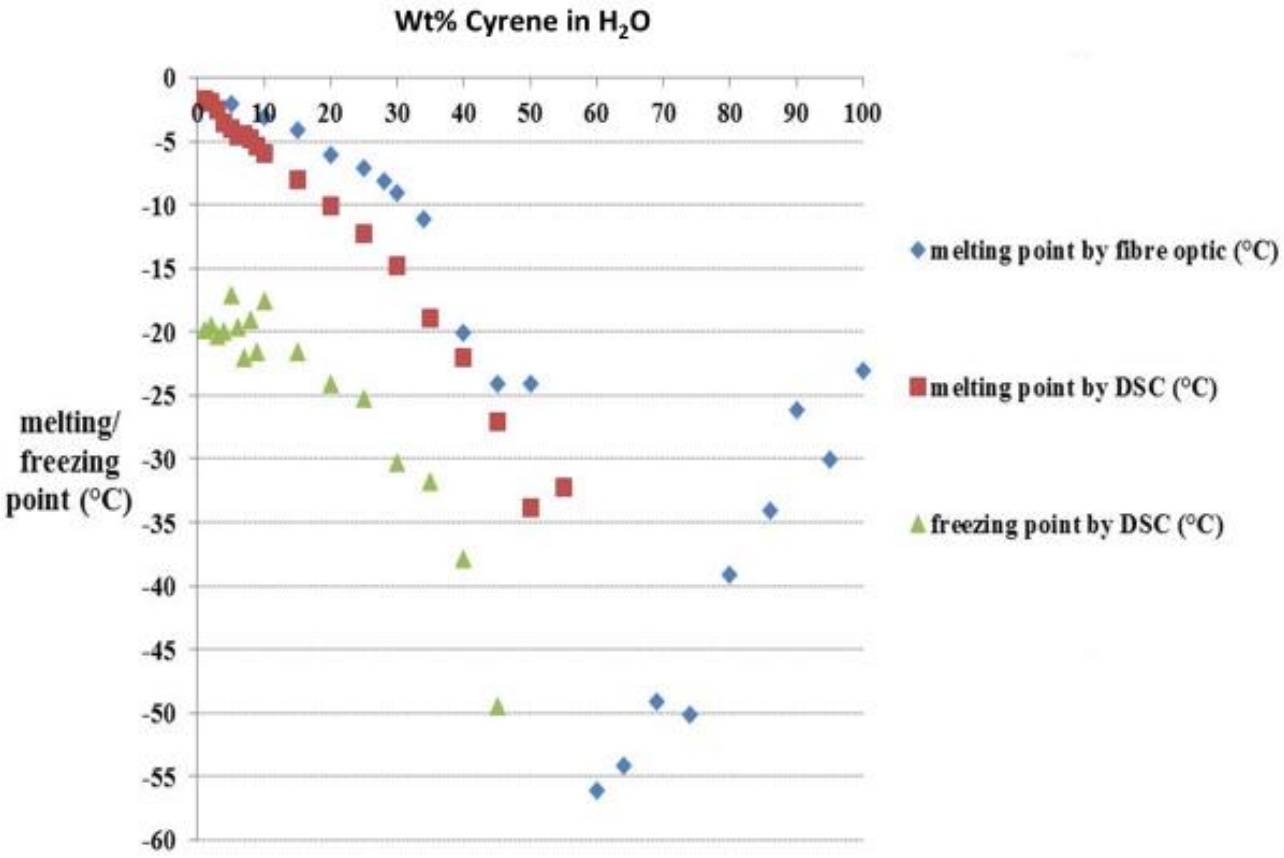

Figure 3.6 Comprehensive graph showing the melting point obtained with fibre optic (in blue), the melting point by DSC (in red), and the freezing point obtained by DSC (in green).

As can be seen from Figure 3.6 the melting points determined by DSC and fibre optic probe follow the same trend albeit some structural deviation is present. The determined freezing points (DSC) are appreciably lower than the melting points (DSC) which is most likely due to supercooling. Irrespective the method, all data suggests the presence of a eutectic point close to -55^{0}C. The Cyrene/geminal diol/water ternary mixture could thus be considered a "**na**tural **d**eep **e**utectic **s**olvent" also known as NADES. Figure 3.7 shows the melting of a frozen 50 wt% Cyrene in water solution which has an apparent high viscosity. During the melting process the temperature is quasi constant and the formed ice is amorphous.[98] This is in accord with the DSC thermogram not displaying any peak related to freezing or melting.

Figure 3.7 Visual on the melting of a cyrene/geminal diol/water ternary mixture with an initial concentration of Cyrene in excess of 50 wt%.

It was attempted to calculate the molecular weight of Cyrene using the DSC determined melting point depression data of the more dilute Cyrene/water combinations following equation 3.1. For this particular purpose the data of the freezing point depression were not used as the thermograms showed clear supercooling of water.[99-101]

$$\Delta T = iK_f m \qquad [\text{Eq.3.1}]$$

Where, ΔT is the difference in temperature, K_f is the cryoscopic constant of water = 1.86 °C kg/mol and **i** is the van 't Hoff factor in this case i=1, and m = the molality of the solution.

Unfortunately this approach failed which probably relates to the simultaneous presence of Cyrene and its geminal diol as well as the complex interaction between the three different components in the ternary mixture – making the system not ideal.

3.4 Calculation of the activity of water

In food science the quantity of water present is an important factor to control the stability and the preservation of most products. The activity of water a_w is a very important parameter to sample the food quality and check for potential microbial spoilage. It basically indicates how tight the water is bound. Products with low activity values are better preserved because the water is unavailable to microbes. The activity of water can also provide information on the structure in solutions. For instance in water sugar solution it is proportional to the quantity of –OH in the solute.

Activity of water	Molarity of solution
1	0
0.992	0.01
0.989	0.03
0.987	0.05
0.985	0.078
0.983	0.1
0.981	0.159
0.976	0.243
0.972	0.324
0.966	0.41
0.964	0.498
0.960	0.59
0.956	0.684
0.952	0.768
0.948	0.87

Table 3.1 The activity data calculated using equation 3.3 (employing the melting point data determined by DSC).

Using the DSC obtained melting point data it was found possible to calculate the activity of water in the ternary Cyrene/geminal diol/water mixture using equation 3.2.[102] (see table 3.1) Because of the presence of super cooling, the melting point values were used for the calculation.

$$\ln a_w = -\frac{\Delta H_f}{R}\frac{(T_f - T)}{T_f T} + \frac{\Delta Cf}{R}\left[\frac{(T_f - T)}{T} - ln\left(\frac{T_f}{T}\right)\right] \qquad \text{Eq.3.2}$$

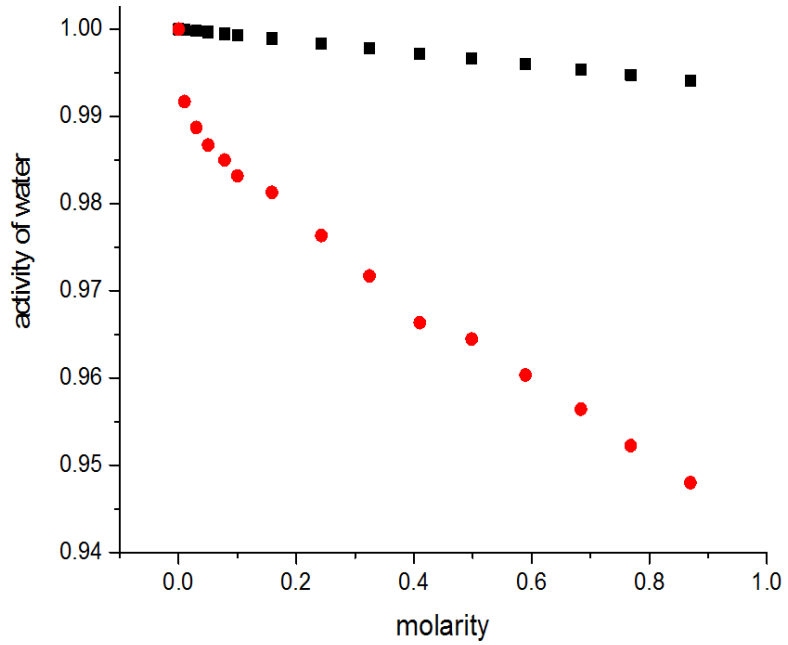

Figure 3.8 Shows the theoretical (black) and the experimental activity (red) of water (in the ternary mixture) against the molarity of the solution obtained using DSC data.

As shown before Cyrene shows a complex behaviour in water.[103-105] From Figure 3.8 a deviation of the linearity is visible for ternary mixtures low in water content. The experimentally measured water activity values (red) point a substantially non-ideal behaviour – as shows from its comparison to the theoretically expected curve (black).

3.5 the Cyrene/geminal diol/water ternary mixture as a chameleon solvent and a switchable hydrotrope

This part concerns a unique application of the Cyrene/geminal diol/H_2O ternary mixtures which has also been submitted (in a different form) to the journal of Green Chemistry (currently under review)

3.5.1 Background of the Cyrene (aprotic) - geminal diol (amphiphilic) - water (protic) system

The dissolution of chemical substances is a corner stone of the chemical industry, with millions of metric tons of solvent consumed per year.[106] Solubility links directly to the properties of the solvent but also the addition of surfactants and hydrotropes to solvents can play an important role.[107,108] Presently, the use of many conventional solvents has come under increasing scrutiny, relating to their strongly negative environmental impacts and often high toxicities.[109] This has reinforced the search for novel solvents, with more benign characteristics. Ideally these are bio-derived i.e. deriving more than 25% w/w of its carbon from bio-based resources.[110] Examples of these are methyl-THF, glycerol, γ-valerolactone, ethylacetate and dihydrolevoglucosenone (Cyrene™).[111,112] The latter is of particular importance as it is a rare example of a bio-derived dipolar aprotic solvent displaying similar characteristics to N-methylpyrrolidone (NMP) and dimethylformamide (DMF), both known reprotoxic solvents.[112]

The creation of solvent systems, comprising two or more (benign) components, has also been reported. Notable examples are (NAtural) Deep Eutectic Solvents [(NA)DES], Low Transition Temperature Solvents (LTTS) and Switchable Solvents (S-S). These have the advantage of being easily tuneable to the application. (NA)DES are formed from a eutectic mixture of two or more solids, which is liquid near to room temperature. Typically they involve Lewis or Brønsted acids and bases, containing a variety of anionic and/or cationic species. (NA)DES has the advantage that they are simple and cheap to make, can be tuned to the application and are generally non-volatile, biodegradable, biocompatible and non-toxic.[113,114] LTTS are similar to (NA)DES but instead of a eutectic melting point, they display a glass transition temperature.[115] Examples of S-S are the reversible decomposition of piperylene sulfone and the one or two component reversible ionic liquids.[116,117] Key to the latter is the reversible conversion of a basic nitrogen into an ammonium by means of CO_2 bubbling.

Surfactants are also often used to increase the solubility of compounds, typically through micellar action. Thereby the core-corona structure is of particular importance: the hydrophobic core

providing for a suitable hydrophobic micro-environment and the hydrophilic corona acting as stabilizer for the hydrophilic part in the aqueous environment.[118] Hydrotropes are small amphiphilic compounds which, at elevated concentrations, are able to enhance markedly the aqueous solubility of hydrophobic compounds.[109] They are generally solids, examples of which are sodium benzoate, pyrogallol and short-chain glycol ethers. They can however also be liquids in which case they are known as "chameleonic solvents" or "solvo-surfactants". These display an amphiphilic character, conferring special solvation abilities to the molecules. Exemplary are the short-chain ethers of mono/di/tri propylene glycols which can dissolve organic substances in water by a hydrotropic mechanism but also by forming monophasic micro-emulsion-like systems. Glycol ethers are though controversial substances due to their suspected/proven toxicity and reprotoxicity.[119] This phenomenon has also been described for ionic liquids, such as [C4MIM][PF6], a molecule which can act as a polar molecule in some situations and as nonpolar molecules in others, depending on the medium.[120] Ionic liquids have also been shown to act as catanionic hydrotropes where the cation and anion synergistically contribute to the solubility of biomolecules in water. The enhanced solubility's were linked to the formation of "ionic liquid-biomolecule" aggregates.[121]

The ability of Cyrene to interact with water, forming its geminal diol (1S,5R)-6,8-dioxabicyclo[3.2.1]octan-4,4-diol) has been reported before but only as intermediates in synthetic protocols.[122] To date, no in depth study on their properties has been reported to date. Herein, a new solvent system, representing the equilibrium between Cyrene, its geminal diol and H_2O is presented. This solvent system behaves akin to a chameleon solvent while displaying tuneable hydrotrope properties.

3.5.2 Description of the Cyrene (aprotic) - geminal diol (amphiphilic) - water (protic) equilibrium.

Figure 3.9_A and Table 3.2 (in appendix) show the composition of the ternary Cyrene, water, geminal diol mixture (hereafter abbreviated as TM-H_2O/D_2O), as determined by ^{1}H NMR spectroscopy (no deuterated solvent present). This is plotted as a function of the initial amount of Cyrene added to water (in wt%) and with both the molar amounts of geminal diol and resulting H_2O (i.e. water that has not engaged in forming the geminal diol) normalized to 1 mol Cyrene. The composition of the mixture can thus be adequately described as [Cyrene normalized moles geminal diol; Cyrene normalized moles H_2O/D_2O] couples. The occurrence of a controllable equilibrium between Cyrene, its geminal diol and H_2O is an interesting phenomenon as it imparts tuneability on the Cyrene solvent. While Cyrene has been classified as a dipolar aprotic solvent, the introduction of water, and the consequent formation of Cyrene's geminal diol, introduces significant polarity in the form of two hydroxyl groups, adding thus hydrogen bonding capacity to the Cyrene molecule. Additionally, the formation of geminal diol introduces equally substantial amphiphilicity. Therefore, and depending on the initial Cyrene/H_2O ratio, a solvent with well-defined hydrophobic/hydrophilic properties can be created.

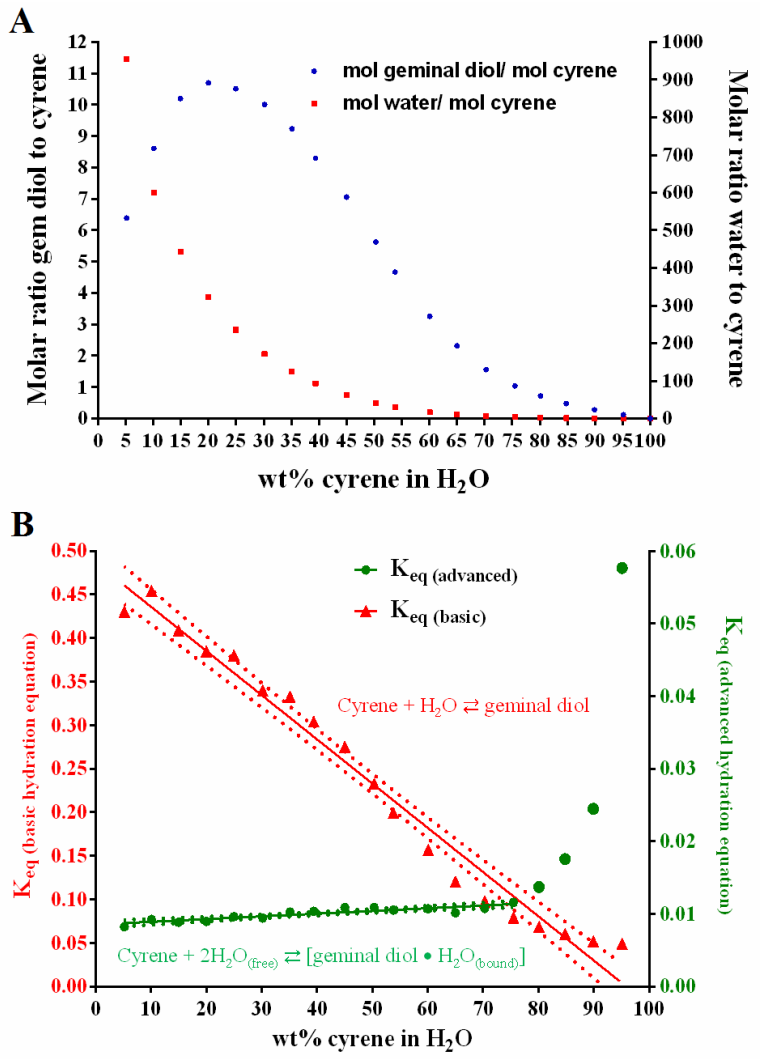

Figure 3.9 A) Composition of the ternary Cyrene/geminal diol/H_2O mixture (TM-H_2O) plotted against the initial amount of Cyrene added to H_2O (in wt%). B) Plots of the equilibrium constant for two different reaction models displayed as a function of the initial wt% of Cyrene in H_2O. T = 298 K.

3.5.3 Stoichiometry of the Cyrene – geminal diol interconversion.

From the data presented in Figure 3.9_A the equilibrium constant (K_{eq}) of the Cyrene hydration reaction was evaluated (Figure 3.9_B and Table 3.3). Two different models for the Cyrene – water interaction/ reaction were evaluated being (a) the intuitive reaction stoichiometry in which Cyrene reacts with one water molecule yielding geminal diol and (b) a reaction stoichiometry in which two water molecules are involved, one reacting with the Cyrene and one hydrogen bonding strongly to the formed geminal diol. Model (a) (Figure 3.9_B, red equation) proved to be insufficient as no constant K_{eq} could be established. Model (b) (Figure 3.9_B, green equation) yielded a near-constant K_{eq} up until 75 wt % Cyrene, making it a more realistic description within this concentration range. However, the drastic increase of K_{eq} after the 75 wt % Cyrene mark, in which zone the amount of water is limited, does suggest that model b does not fully capture the Cyrene – geminal diol interconversion.

3.5.4 Density & viscosity: evidence for a hydrogen bond network in the ternary mixture.

A) Density

The experimental densities (EDs) of the H_2O and D_2O based TMs are shown in Figure 3.10 and tabulated in tables 3.4-3.5 (in appendix). Unusually, the water addition to Cyrene is found to increase the TM-H_2O density from 1.2517 g mL^{-1} (pure Cyrene) to 1.2672 g mL^{-1} at ~ 80 wt% Cyrene in H_2O. This corresponds to a TM-H_2O composition of [0.72: 2.31] (Table 3.2 in appendix). The EDs of TM-D_2O increase somewhat more pronounced than observed for TM-H_2O, reaching a maximum value of ~1.304 g mL^{-1} at ~70 wt% Cyrene in D_2O. This corresponds, by interpolation (Table 3.6 in appendix), to a TM-D_2O composition of [~1.64: ~6.17]. The density data, and particularly the difference between the densities of the TM-H_2O and TM-D_2O systems, suggests for a strong influence of hydrogen bonding: as water is added to the Cyrene, the formed geminal diol engages strongly in hydrogen bonding, countering the dilution effect of the water. However, SAXS (Figure 1A in appendix) and imaging by polarized light microscopy failed to discern any structural organization of the TMs beyond the molecular length scale. On the other hand ESI mass-spectrometry did indicate the presence of geminal diol monomers and dimers (Figure 2A in appendix). Taken all together, the hydrogen bonding in TM does not seem to lead to apparent long range molecular complexes.

B) Viscosity

The viscosity of TM-H_2O was also determined (Figure 3.10 and Table 3.7 in appendix). Contrary to the density, the viscosity changes markedly with increasing water content. The highest viscosity of 21.16 cP is observed at ~75 wt% Cyrene in H_2O – representing a TM-H_2O composition of [1.04: 3.68]. Highest viscosity is thus observed in the same region as highest density. Notably this region is characterized by the presence of similar quantities of Cyrene and its geminal diol. The dissolution of a variety of compounds in a range of TMs-H_2O was evaluated. Figure 3.11A/B (and Tables 3.8 & 3.9 in appendix) shows the dissolution of aspirin, salicylic acid, ferulic acid, phthalic acid, caffeine and mandelic acid as a function of the initial Cyrene wt% in H_2O.

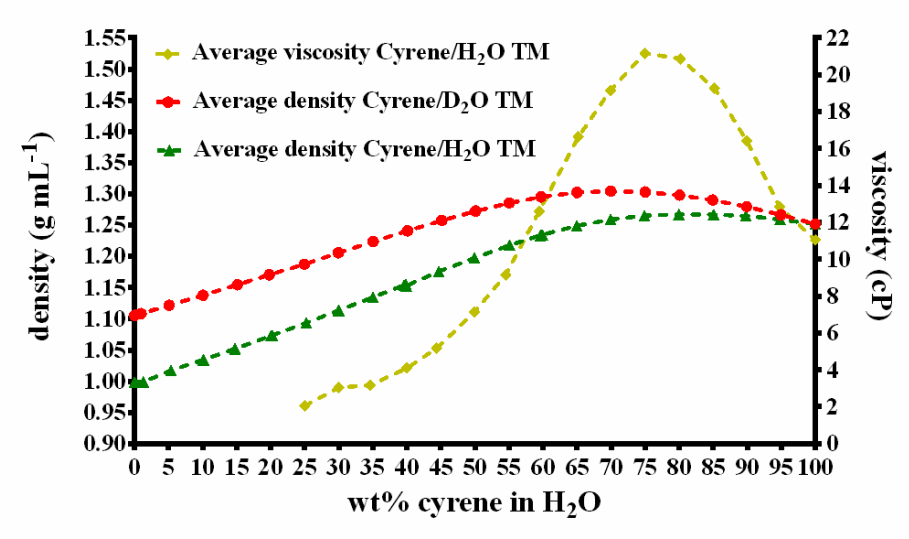

Figure 3.10. The experimental densities of TM-H_2O and TM-D_2O [T = 295.15 K] and the experimental viscosities of TM-H_2O [T = 298 K] - all as a function of the initial wt% Cyrene added to H_2O/D_2O.

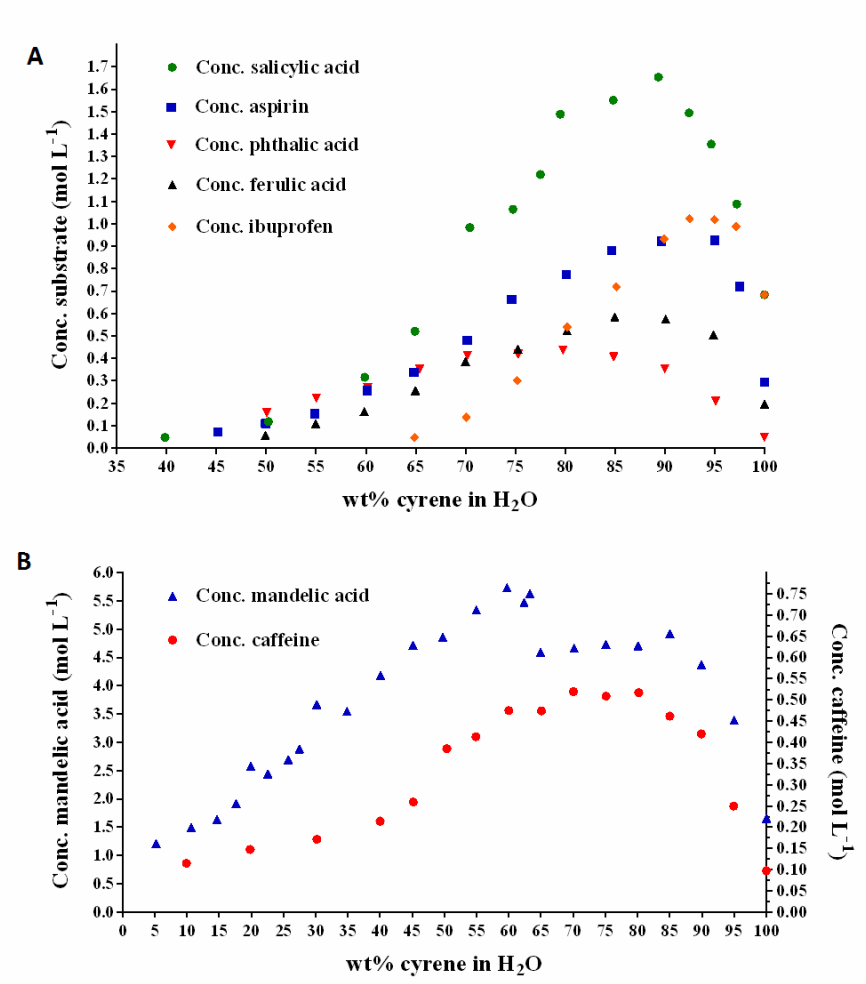

Figure 3.11 A) Solubility of aspirin, salicylic acid, phthalic acid, ferulic acid and ibuprofen. B) Solubility of caffeine and mandelic acid; all displayed as a function of the TM-H_2O.

3.5.5 Geminal diol as a hydrotrope

From the water rich side, characteristic hydrotropic behaviour can be observed for the first four compounds (aspirin, salicylic acid, ferulic acid and phthalic acid) with a sudden solubilization onset at ~ 45-50 wt% Cyrene in H_2O (Figure 3.11 and Tables 3.8/3.9 in appendix). Specific to salicylic acid two additional hydrotropic onsets can be observed at respectively 70 and 80 wt% Cyrene in H_2O. These reflect likely the influence of the changing polarity of the TM-H_2O system on the salicylic acid. In the case of caffeine the TM-H_2O acts as a mixture of three different solvents (Cyrene, H_2O and geminal diol) up to 40 wt% Cyrene in H_2O, there linearly and mildly increasing the solubility. This is then followed by a hydrotropic increase of the caffeine solubility at the 45 wt% Cyrene in H_2O mark, again exhibiting cooperative solubilization. As to the more water soluble mandelic acid, Cyrene and geminal diol act merely as co-solvents, leading to a linear increase of solubility in its presence.

3.5.6 Geminal diol formation plays a dominant role in hydrotropy.

With exception of salicylic acid, the maximum solubility of all tested compounds reach a plateau concentration, covering a range of Cyrene/H_2O compositions (Table 3.10 in appendix). For instance, the maximum solubility of aspirin is observed between 90-96 wt% Cyrene in H_2O while ibuprofen reaches it between 92.5-97 wt% Cyrene in H_2O. No immediate relationship can be discerned between the ranges of maximum dissolution and any physical property of the solutes (e.g. solubility in water/Cyrene, Kow). This accentuates further the dominant role of the amphiphilic geminal diol on the observed solute solubilities in TM-H_2O. In Table 3.10 (in appendix) the observed increases of the solute solubilities for the tested compounds, due to the geminal diol switchable hydrotropic effect, are depicted. It is shown that this can reach up to a factor of 10000 for very slightly soluble solutes in H_2O.

3.5.7 Geminal diol as a chameleon solvent

From the Cyrene rich side the addition of small amounts of H_2O to Cyrene (5-20 wt% H_2O) equally leads to pronounced increases in the solubilities of the tested solutes (Figure 3.11 and Tables 3.8/3.9 in appendix). In Table 3.11 (in appendix) the increase of solute solubility due to the presence of the geminal diol chameleon solvent is shown to reach up to a factor of 8.9. Again no immediate relationship can be derived between any of the solutes' properties and their maximum solubility, in absolute number or in range, in TM-H_2O.

3.5.8 The influence of the solute on the Cyrene – geminal diol – water equilibrium

The effect of the solutes on the TM-H_2O equilibrium was also investigated (Figure 3.12). Interestingly, the hydrophobic solutes do not have any appreciable effect on the geminal diol/Cyrene ratio. In contrast, the more water soluble mandelic acid does affect the equilibrium, its presence inducing an appreciable reduction of the geminal diol content. This is tentatively

attributed to a favourable interaction between Cyrene and mandelic acid, affecting the ease of formation of the geminal diol.

3.5.9 The influence of the solute on the Cyrene – geminal diol – water equilibrium

Effective recovery of the substrates can be achieved by shifting the TM-H_2O equilibrium to a zone in which the substrate is not soluble. This can be realized by adding the necessary amount of water to reach, for example, a water concentration below 50 wt%, at which many of the above discussed aromatic substrates are not soluble (Figures 3.12 & 3.13 A/B). Alternatively, the removal of the H_2O component using vacuum could also be considered provided though the substrate has a low/negligible solubility in pure Cyrene. Lowering or increasing the temperature may also aid the precipitation process as temperature NMR studies of the TM-H_2O equilibrium show that a decrease/increase in temperature favours respectively the geminal diol or Cyrene (Figure 3A and 4A in appendix), thus changing the polarity of the overall mixture.

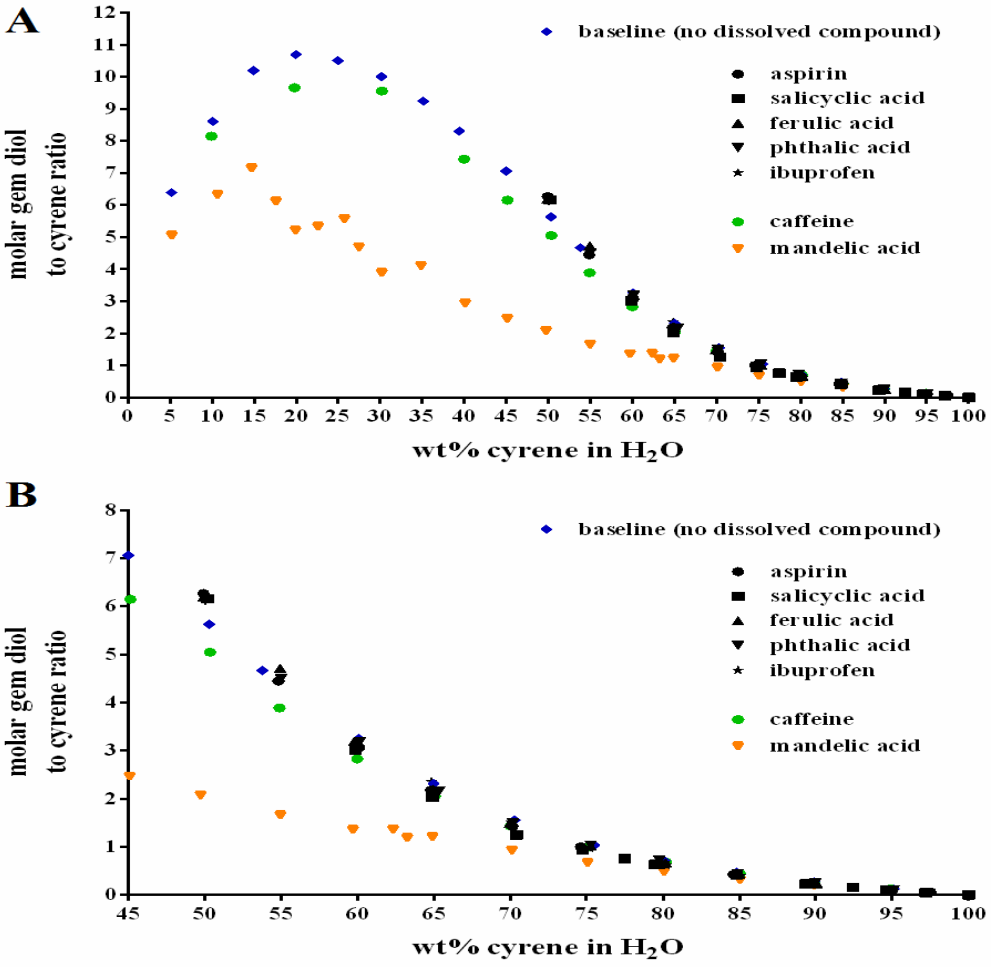

Figure 3.12 A) Plot of the molar geminal diol/Cyrene ratio in the presence of a range of solutes. B) detail of (A) limited to the 45-100 wt% Cyrene in H_2O range composition.

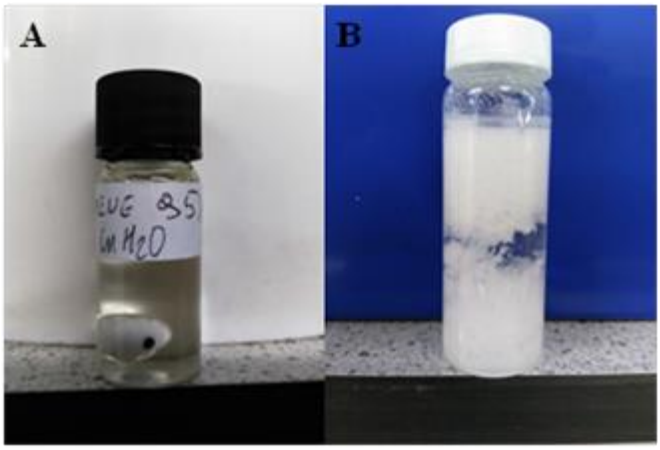

Figure 3.13 A) Saturated solution of aspirin in 95 wt% Cyrene in H_2O. B) Precipitated aspirin from 'solution A' upon the addition of water.

Conclusions

In this work and in depth investigation of Cyrene and Cyrene hydrate was performed using a range of analytical techniques.
On the one side significant effort was spent trying to elucidate the appearance of a double carbonyl group stretch in the infrared spectrum of liquid Cyrene. It was established that this is likely related to intermolecular interactions between Cyrene molecules e.g. hydrogen bonding. The hypothesis of a Fermi resonance could be largely excluded as the relevant IR/Raman spectroscopy experiments were unsupportive of its occurrence. Calculation of the IR spectra provided additional evidence for the existence of Cyrene dimers/oligomers. Likewise also the calculation of the entropy of vaporization of Cyrene at boiling point pointed in the same direction as a clear positive deviation of Trouton's rule was established.

The Cyrene hydrate was fully characterized through NMR spectroscopy techniques combined with precision measurements of density and viscosity. It was established that a ternary mixture is formed comprised of defined amounts of Cyrene, geminal diol and free water. The equilibrium is complex and probably involves more than just one water molecule. Generally interesting phenomena were observed when the initial content of Cyrene in water exceeds 50 wt%. In this zone the density remains very high and a (relatively) strong increase in the viscosity can be observed – the maxima situating themselves around the 75 wt% initial Cyrene content. At this special point equimolar amounts of Cyrene and its geminal diol are present accompanied from ~4 water molecules. Importantly it was found that on the one side the ternary mixture, and particularly the geminal diol, acts as a hydrotrope significantly enhancing the solubility of a range of pharmaceutical molecules from the 45-50 wt% Cyrene mark onwards. In the case of ibuprofen this concerned an increase in solubility with a factor of 10000. From the Cyrene rich side the ternary mixture works as a chameleon or hidden solvent – the appearance of the amphiphilic geminal diol there leading to solubility increases up to 9-fold.

Applications for the ternary mixture may be wide-ranging. In the pharmaceutical industry the solubilization of drugs is critical and many of them are virtually insoluble or poorly soluble in water.[123] Exact “hydrotropy” is one of the recognized techniques available for resolving these solubility issues.[124,125]

Materials, methods and instrumentation

Double distilled dihydrolevoglucosenone (Cyrene) was provided by the Circa company and used as is.

^{1}H and ^{13}C NMR spectroscopy experiments were recorded using a special probe allowing for recording the spectra in the absence of a deuterated solvent. It was determined that a relaxation delay of 20s allowed for reliable quantification of the ^{1}H and ^{13}C NMR signals. To aid with the quantification the NMR tubes were filled to ~4 cm height in an as consistent manner as possible. Composition of the TM-H_2O mixture was determined from ^{1}H NMR spectroscopy data while the solubility data was recorded from ^{13}C NMR spectroscopy data as to avoid the higher complexity of the ^{1}H NMR spectroscopy data.

All Cyrene-H_2O mixtures were prepared to a total volume of 2 mL and stirred at 400 rpm for 30 minutes. This allows in all cases to obtain a homogeneous solution. Inhomogeneity of the Cyrene/water mixtures is commonly observed for samples rich in Cyrene but disappearing through continued stirring (30 min is ample) or gentle heating (e.g. in the hand). To determine the solubility, saturated solutions were prepared and stirred for 35 minutes at 400 rpm. This is followed by room temperature centrifugation at 3500 rpm. The supernatant was pipetted out, filtered over cotton if still cloudy, and added into an NMR tube to a liquid height of 4 cm.

NMR spectra were taken on a Bruker AVIIIHD500 [500 MHz]. The Bruker runs Topspin 3.5. and uses a TBO triple resonance probe for HFX. To prepare the spectrometer before running unlocked samples in H_2O; a standard sucrose sample in 90%/10% H_2O/D_2O is used to set the field, tune and do an initial shim using the Topshim program which uses deuterium. Each sample is then tuned, and then gradshimmed via the proton signal before acquiring the spectra.

The ESI spectrum was obtained through a Bruker microTOF time of flight mass spectrometer with ESI source.

The densities were determined on an ANTON PAAR DSA 5000 vibrating tube density meter at 295.15 K. The amount of sample in the measuring cell was about 3 mL. Each data point was calculated from the average of 8 runs. The temperature accuracy given by the manufacturer was ±0.001 K. Samples were prepared in various concentrations, mixing the desired amounts of Cyrene and water (H_2O/D_2O) followed by stirring (10 min), to a total volume of 5 mL. Subsequently the so obtained mixtures are degassed using ultrasounds for 5 min. Before analysis the instrument is calibrated with distilled ultrapure water.

The viscosity of the Cyrene/water mixtures was measured with a programmable Brookfield rotational rheometer RVDV-II+Pro (cone and plate version) connected to a cryostat to control the samples (temperature accuracy ±1 K). A Brookfield silicone fluid (97 mPa s, 298 K) was used as a NIST-traceable viscosity standard. Samples were prepared by mixing the desired amounts of Cyrene and water to a total volume of 2 mL. This was followed by 10 minutes stirring and an ultrasound mediated degassing step (3 min). The viscosity data were collected at 298 K using a CP-40 cone. For all systems 10 runs were conducted for each data point. The sample volume used for each

experiment was 0.5 mL. All fluids measured showed a Newtonian behavior at 298 K within the range of shear rate examined (7.50- 712.50 s^{-1}).

Small-angle X-ray diffraction was performed using a Bruker D8 Discover equipped with a temperature-controlled, bored graphite rod furnace, custom built at the University of York. The radiation used was copper Kα (λ = 0.154056 nm) from a 1 µS microfocus source. Diffraction patterns were recorded on a 2048 × 2048 pixel Bruker VANTEC 500 area detector. Samples were filled into 1 mm capillary tubes. Diffraction patterns were collected at 300.8 K and the data processed using the DIFFRAC.EVA software. The acquisition time for each sample was 30 min.

Fourier transform infrared spectroscopy of Cyrene and Cyrene-water solution were carried out using a Bruker vertex 70 FT-IR spectrometer fitted with Specac Golden Gate ATR. The instrument was equipped with a DigiTect^{TM} DLATGS detector with integrated preamplifier scanning in the range over a wavelength range of 4000-400 cm^{-1} with a resolution of 1 cm^{-1}. All the spectra were collected using OPUS 5.5 software and calculated from an average of 64 scans. FTIR of Cyrene in gas phase were performed with a self-made environmental chamber.

In situ FTIR were collected on a Mettler Toledo React IR ic10 using a Silica ATR probe and an icIR software analysis system in the range of 4000-400 cm^{-1} with a resolution of 4cm^{-1}. The probe was placed in the middle of the solution, which was constantly stirred by a magnetic bar, and the spectra were collected in situ under flow of nitrogen.

IR analysis in temperature of Cyrene were performed using a Bruker Equinox 55 FT-IR spectrometer with software OPUS 5.5.The spectrometer resolution was 1 cm^{-1} and set at 64 scans per spectrum. The environmental chamber for temperature was self-made.

Differential scanning calorimetry analysis were measured on a DSC Q2000 calorimeter. The samples (14 mg) were weighed into a open aluminium anodized pan and sealed with a hermetic lid. DSC measurements were recorded against an empty aluminium pan (with hermetic lid) as reference, under a flow of nitrogen gas (150 ml/min) using the following method:

1) equilibrate at 20 °C

2) ramp 5 °C/min to -70 °C

3) ramp 15 °C/min to 20 °C (x 2 times)

DLS measurements were conducted at 25 °C using a Zetasizer Nano ZS analyzer with integrated 4 mW He−Ne laser, λ = 633 nm (Malvern Instruments Ltd., U.K.). The Cyrene water solutions were measured after mixing and degassed in ultrasound. All measurements were carried out using cells (DTS0012) in five replicate measurements.

Raman spectra were recorded by a dispersive confocal Raman spectrometer (Horiba XploRA). A green laser diode with a wavelength of 532 nm, a nominal output power of up to 25 mW and a spot size of approx. 1 µm was used as the excitation source. The Raman signal was detected by a silicon CCD detector and 90 scans were collected with an exposure time of 10 s. The spectral range varied from 400 to 4000 cm^{-1} with an instrumental spectral resolution of 1–2 cm^{-1}.

Chapter 4: *Reference*

References

1. Sherwood J., Chem. Commun., 2014, 50(68), 9650-9652.
2. Clark J. H., Int. J. Mol. Sci., 2015, 16(8), 17101-17159.
3. Anastas P. T., Warner J. C., in Green chemistry: Theory and practice, Oxford University Press, Oxford, UK, 1998, pp.29-56.
4. Kerton F. M., and Marriott Ray, In Alternative solvents for green chemistry. No. 20, Royal Society of chemistry, 2013, ch.1.2.
5. Kerton F. M., and Marriott Ray, In Alternative solvents for green chemistry. No. 20, Royal Society of chemistry, 2013, ch.1.3.
6. Reichardt C., Chem. Rev., 1994, 94(8), 2319-2358.
7. Makitra R. G., Reichardt C., Solvents and Solvent Effects in Organic Chemistry, Weinheim: Wiley-VCH, 2003.
8. Buckingham A. D., Fowler P. W., Hutson J. M., Chem. Rev., 1988, 88(6), 963-988.
9. Huyskens P. L., luck. W.A.P., Zeegers-Huyskens T., Intermolecular forces: an introduction to modern methods and results, Springer Science & Business Media, 2012.
10. Adams Dave J., Dyson Paul J., Tavener Stewart J., In Chemistry in alternative reaction media. John Wiley & Sons, 2005, p.14.
11. Shinoda K., In Priciples of solution and solubility, Marcel Dekker inc., New York, 1978, p.55.
12. Murrell and Jenkins, Properties of liquids and solutions,Wiley, second edition, New York, 1994.
13. Hildebrand and Scott, In Regular solutions, prentice-hall inc., 1962, pp167.
14. A.A. Tager, L.K. Kolmakova, vysokomol. Soed. A22, 1980, 483.
15. Wypych, in Handbook of solvents, vol1, ChemTec Publishing, Toronto, 2014, pp121.
16. Shinoda K., In Principles of solution and solubility , marcel dekker inc , new York 1978 , pp57-60.
17. Wypych, In Handbook of solvents, vol1, ChemTec Publishing, Toronto ,2014, pp122.
18. Abbott S., and Charles M. Hansen, Hansen solubility parameters in practice. Hansen-Solubility, 2008.
19. Nigam, Shalini, and Sarah Rutan. Principles and applications of solvatochromism, Applied Spectroscopy, 2001, 55.11, 362A-370A.
20. Yizhak M., The properties of solvents. Vol. 16. Chichester, Wiley, 1998.
21. Dimroth K., Reichardt C., Siepmann T., andBohlmann F., Liebigs Ann. Chem., 1963,661,1.
22. Reichardt C., Leibigs Ann. Chem., 1969, 727, 93.
23. Kamlet M. J. and Taft R. W., J. Am. Chem. Soc., 1976, 98, 377.
24. Kamlet M. J. and Taft R. W., J. Am. Chem. Soc., 1976, 98, 377-383.
25. Kamlet M. J., Abboud J. L., and Taft R. W., J. Am. Chem. Soc., 1977, 99, 6027.
26. Kerton, Fl., and Marriott R., In Alternative solvents for green chemistry. No. 20. Royal Society of chemistry, 2013. Ch.1.1.

27. Court G. R., Lawrence C. H., Raverty W. D. and Duncan A. J., US Pat., 2012/0111714 A1, 2012.
28. Alavianmehr M. M., J. Mol. Liq., 2016 ,218, 332-341.
29. Abbott S., Booth J. J., Shimizu S., Green Chem., 2017, 19, 68-75.
30. Booth J. J., Abbott S., Shimizu S., j. Phys. Chem. B, 2012, 116, 14915-14921.
31. Shimizu S., Booth J. J., Abbott S., Phys. Chem. Chem. Phys., 2013, 15, 20625-20632.
32. Booth J. J., Omar M., Abbott S., Shimizu S., Phys. Chem. Chem. Phys., 2015, 17, 8028-8037.
33. Lowe John P., Peterson Kirk, In Quantum chemistry, Academic Press, 2011, ch.13, p.429.
34. Schrader B., in Infrared and Raman spectroscopy: methods and applications, VCH, Weinheim, 1995, p.39-41.
35. Mueller Michael P., Fundamentals of quantum chemistry: molecular spectroscopy and modern electronic structure computations, Springer Science & Business Media, 2001.
36. Herzberg Gerhard, Molecular spectra and molecular structure, Vol 2, Malabar, 1988.
37. Griffiths David J., Introduction to quantum mechanics. Cambridge University Press, 2016.
38. Herzberg Gerhard, In Molecular spectra and molecular structure, Vol. 1. Krieger Pub. Co. second edition, 1988, p.75.
39. Hollas J.M., in High resolution spectroscopy, Wiley, second edition, 1998, p. 172.
40. Atkins, in Physical Chemistry, Freeman Company, New York, eighth edition, 2006.
41. Banwell, in Fundamentals of Molecular Spectroscopy, McGraw-Hill Book Company, London, 1983, p.77.
42. Hollas J.M., in High resolution spectroscopy, wiley, second edition, 1998, p.165.
43. Morse potential, draw by Mark Somoza March 26, 2006, https://commons.wikimedia.org/wiki/File:Morse-potential.png (accessed April 2017). Accessed April 2017
44. Hollas J.M., in High resolution spectroscopy, Wiley, second edition, 1998, p.246.
45. Banwell, In Fundamentals of Molecular Spectroscopy, McGraw-Hill Book Company, London, 1983, p.94.
46. Banwell, In Fundamentals of Molecular Spectroscopy, McGraw-Hill Book Company, London, 1983, pp.95-97.
47. Hollas J.M., in High resolution spectroscopy, Wiley, second edition, 1998, p.240.
48. Herzberg Gerhard, in Molecular spectra and molecular structure, Vol. 1, Krieger Pub. Co., second edition, 1988, p.14.
49. Herzberg Gerhard, in Molecular spectra and molecular structure, Vol. 2, Krieger Pub. Co. second edition, 1988, p.216.
50. Hollas J.M., in High resolution spectroscopy, Wiley, second edition, 1998, p.248.
51. Hollas J.M., in High resolution spectroscopy, Wiley, second edition, 1998, p.249.
52. Bellamy L., The Infra-red Spectra of Complex Molecules, Springer, 1975.
53. Yaylayan V. A. and Ismail A. A., Carbohydr. Res., 1995, 276, 253-265.
54. Reichardt C., Welton T., in Solvents and solvent effects in organic chemistry, John Wiley & Sons, fourth edition, 2010, pp.438.
55. Fried Stephen D., Bagchi Sayan, and Boxer Steven G., J. Am. Chem. Soc., 2013, 135(30), 11181-11192.

56. Chen Yujing , Morisawa Yusuke, Futami Yoshisuke, Czarnecki M., Hai-Shui Wang, Ozaki Yukihiro, J. Phys. Chem. A , 2014, 118(14), 2576-2583.
57. Kashid Somnath M, Bagchi Sayan, J. Phys. Chem. Lett., 2014, 5(18), 3211-3215.
58. Bervelt J.P., Ottinger R., Peters P.A., Reisse J., Chiurdoglu G., Spectrochim. Acta, Part A, 1968, 24(9), 1411-1420.
59. J.F.Bertran, Ballester L., Dobrihalova L., Sánchez N., Arrieta R., Spectrochim.Acta Part A, 1968, 24(11), 1765-1776.
60. Yaylayan Varoujan A. , Ismail Ashraf A., Carbohydr. Res., 1995, 276(2), 253-265.
61. Court G. R., Lawrence C. H., Raverty W. D. and Duncan A. J., US Pat., 2012/0111714 A1, 2012.
62. Bruttel P., Schlink R., Water Determination by Karl Fischer Titration, Metrohm Ltd., CH-9101 Herisau, Switzerland, 2003.
63. Rijs A. M., Kabelac M., Abo-Riziq A., Hobza P., de Vries M. S., ChemPhysChem, 2011, 12, 1816–1821.
64. Theophanides Theo M., Infrared and Raman spectroscopy of biological molecules : proceedings of the NATO Advanced Study Institute held at Athens, Greece, August 22-31, 1978; D. Reidel Pub. Co. ,series C, Dordrecht, Holland , vol 42 ,1979.
65. Allen G., Ellington P. S., and Meakins G. D., J. Chem. Soc. (Resumed) 1960, 1909-1912.
66. Wei Qiang, J. Mol. Liq., 2013, 177, 225-228.
67. Jeffrey G. A., Saenger, Hydrogen Bonding in Biological Structures, Springer-Verlag W., Berlin, 1991.
68. Scheiner S., Hydrogen Bonding: A Theoretical Perspective, Oxford University Press, New York, 1997.
69. Nyquist R.A. , Vib. Spectrosc, 1994, 7(1), 1-29.
70. Silverstaein, Webster, in Spectrometric identification of organic compound, Wiley, seventh edition, 2005, ch.2, pp.76-77.
71. Stuart B., in Infrared spectroscopy, Wiley, 2004, pp. 12.
72. Schrader B., in Infrared and Raman spectroscopy methods and applications, VCH, first edition , 1995, pp.32-33,226.
73. Atkins P. W., Molecular Quantum Mechanics, Oxford University Press, 1970.
74. Guillory William, Introduction to Molecular Structure and Spectroscopy, Allyn & Bacon Inc., Boston, 1977.
75. Struve Walter, Fundamentals of Molecular Spectroscopy, Wiley, 1989.
76. Kondratyuk Petro, Spectrochim. Acta, Part A , 2005, 61(4), 589-593.
77. Bier K. D., Jodl H. J., J. Chem. Phys, 1987, 86(8), 4406-4410.
78. Socrates G., in Infrared and Raman Characteristic group frequencies, Wiley, 2001, pp. 116-117.
79. Peddle G.J.D., J. Organomet. Chem., 1968, 14(1), 115-121.
80. Michell A. J., and Higgins H. G., Tetrahedron, 1965, 21.5, 1109-1120.
81. Yatsyna Vasyl, Phys. Chem. Chem. Phys., 2016, 18.8, 6275-6283.
82. Reisse J., Bervelt J.P., Cuvelier C., Ottinger R. , Peters Pa., Tetrahedron, 1970, 26(11), 2563-2573
83. Al-Jallo Hikmat N., and Al-Azawi Fatin N.. Spectrochim. Acta, Part A: Molecular Spectroscopy, 1978, 34.7-8 , 819-823.
84. Cataliotti R., Jones R.N., Spectrochim. Acta, Part A, 1971, 27(9), 2011-2013.

85. Vaz PD, Ribeiro-Claro Pja, J. Phys. Chem. A, 2003, 107(32), 6301-6305.
86. Bertrán José Fernández , Ballester Lourdes, Spectrochim. Acta, Part A, 1983, 39(2), 123-125.
87. Ortiz E. , Bertran J.Fernández, Ballester L. , Spectrochim. Acta, Part A, 1971, 27(9), 1713-1720.
88. Sherwood J., De Bruyn M., Constantinou A., Moity L., Mcelroy C.R., Farmer T. J., Duncan T., Raverty W., Hunt A. J., Clark J., Chem. Comm., 2014, 50(68), 9650
89. Nash Leonard K., J. Chem. Educ., 1984, 61(11), 981.
90. Bowden S.T., J. appl. Chem., 1954, DOI: 10.1002/jctb.5010040108
91. Atkins, Physical chemistry, oxford university press, 1978.
92. Screttas Constantinos G., Heropoulos Georgios A., and Steele Barry R., J. Chem. Soc. Faraday Trans., 1996, 92.10, 1717-1719.
93. Jorly Joseph, Eluvathingal D Jemmis , J. Am. Chem. Soc., 2007, 129(15), 4620-32.
94. Nolasco Mariela M., Vaz Patrícia M.,Vaz Pedro D., RibeiroClaro Paulo J.A., Chem. Phys. Lett., 2012, 551, 86-91.
95. Reading Mike, and Hourston Douglas J., In Modulated temperature differential scanning calorimetry: theoretical and practical applications in polymer characterisation. Vol. 6. Springer Science & Business Media, 2006.
96. Brown Herbert C., Fletcher Roslyn Silber, Johannesen Rolf B., J. Am. Chem. Soc., 1951, 73(1), 212-221.
97. Fairbrother J. E., Anal. Profiles Drug Subs., 1973, 2, 85-143.
98. Physics Today, 2003, 56, 6, 40; DOI: http://dx.doi.org/10.1063/1.1595053
99. Inoue Takeshi, Tsujii Kaoru , Okamoto Kikuhiko , Toda Kiyoshi, J. Invest. Dermatol., 1986, 86(6), 689-693.
100. Laidler K. J., Meiser J. H., Physical Chemistry, Houghton Mifflin, Boston, 2nd ed., 1995; Ch. 5, p.241.
101. Zavitsas Andreas A., J. Phys. Chem. B, 2001, 105(32), 7805–7817.
102. Miyawaki, Akiko Saito, Takeshi Matsuo, Kozo Nakamura, Biosci. Biotech.Biochem., 1997, 61(3), 466-469.
103. Alzamora Stella M., Chirife Jorge, Gerschenson Lía N., Food res. Int., 1994, 27.1, 65-67.
104. A.Higuchi, T. Iijima, Polymer, 1985, 26, 1833-1837.
105. Zimmerman Robert J., J. Biochem. Biophys. Methods , 1993, 26.1, 61-70
106. Clark J. H., Farmer T. J., Hunt A. J., Sherwood J., Int. J. Mol. Sci., 2015, 16, 17101-17159.
107. Correa N. M., Silber J. J., Riter R. E. and Levinger N. E., Chem. Rev., 2012, 112, 4569-4602.
108. Eastoe J., Hatzopoulos M. H. and Dowding P. J., Soft Matter, 2011, 7, 5917-5925.
109. Byrne F. P., Jin S., Paggiola G., Petchey T. H. M., Clark J. H., Farmer T. J., Hunt A. J., McElroy C. R. and Sherwood J., Sustain. chem. process., 2016, 4.
110. Bio-based solvents, http://www.esig.org/en/regulatory-information/biosolvents). Accessed April 2017
111. Gu Y. L. and Jerome F., Chem. Soc. Rev., 2013, 42, 9550-9570.

112. Sherwood J., De Bruyn M., Constantinou A., Moity L., McElroy C. R., Farmer T. J., Duncan T., Raverty W., Hunt A. J. and Clark J. H., Chem. Commun., 2014, 50, 9650-9652.
113. Alonso D. A., Baeza A., Chinchilla R., Guillena G., Pastor I. M. and Ramon D. J., Eur. J. Org. Chem. , 2016, 612-632.
114. Paiva A., Craveiro R., Aroso I., Martins M., Reis R. L. and Duarte A. R. C., Acs Sustainable Chemistry & Engineering, 2014, 2, 1063-1071.
115. Francisco M., van den Bruinhorst A., Kroon M. C., Angew. Chem. Int. Ed., 2013, 52, 3074-3085.
116. Pollet P., Eckert C. A. and Liotta C. L., Chem. Sci., 2011, 2, 609-614.
117. Jessop P. G., Mercer S. M. and Heldebrant D. J., Energy Environ. Sci., 2012, 5, 7240-7253.
118. Bhat P. A., Rather G. M. and Dar A. A., J. Phys. Chem. B, 2009, 113, 997-1006.
119. Molinier V., Aubry J.-M., in Carbohydrate Chemistry, The Royal Society of Chemistry, 2014, vol. 40, ch. 4, pp. 51-72.
120. Batista M. L. S., Neves C., Carvalho P. J., Gani R. and Coutinho J. A. P., J. Phys. Chem. B, 2011, 115, 12879-12888.
121. Claudio A. F. M., Neves M. C., Shimizu K., Lopes J. N. C., Freire M. G. and Coutinho J. A. P., Green Chem., 2015, 17, 3948-3963.
122. Pecka J., Stanek J. andCerny M., Collect. Czech. Chem. Commun., 1974, 39, 1192-1209.
123. Khadka P., Ro J., Kim H., Kima I., Kima J., Kima H., Choa J., Yunb G., Leea J., Asian J. Pharm. Sci., 2014, 9, 304–316.
124. Brahmankar D., Jaiswal S., Biopharmaceutics and Pharma- cokinetics: A Treatise, Vallabh Prakashan, India, third ed., 2011.
125. Dhapte, Vividha, and Piyush Mehta, St. Petersburg Polytechnical University Journal: Physics and Mathematics, 2015, 1.4, 424-435.

Appendix

Table 3.2 Composition of the Cyrene/gem diol/water ternary mixture (mol geminal diol and mol H_2O both normalized to 1 mol Cyrene). [298 K]

wt% Cyrene in H_2O	mol geminal diol/ mol Cyrene	mol H_2O/ mol Cyrene
5.18	6.39	955.114
10.09	8.61	600.554
14.95	10.20	442.901
19.99	10.70	322.355
24.97	10.51	235.453
30.15	10.01	171.430
35.11	9.24	125.336
39.40	8.30	93.223
45.00	7.06	63.107
50.30	5.63	41.008
53.80	4.67	29.978
60.10	3.26	16.871
65.00	2.32	10.412
70.30	1.56	6.132
75.50	1.04	3.675
80.10	0.72	2.313
84.80	0.48	1.4
89.90	0.28	0.742
95.10	0.12	0.293
100.00	0.00	0.00

Table 3.3 Concentration data of the different components in the ternary mixture and calculated Keq. [298 K]

wt% Cyrene in H_2O	M Cyrene (mol L^{-1})	M gem diol (mol L^{-1})	M H_2O (mol L^{-1})	Keq (basic)	Keq (advanced)
5.18	0.017	0.393	53.009	0.430	0.008
10.09	0.034	0.779	50.732	0.454	0.009
14.95	0.0590	1.167	48.443	0.409	0.009
19.99	0.089	1.582	46.005	0.385	0.009
24.97	0.121	2.008	43.499	0.380	0.01
30.15	0.1766	2.447	40.790	0.340	0.009
35.11	0.228	2.887	38.051	0.333	0.010
39.45	0.301	3.256	35.570	0.304	0.010
44.96	0.418	3.715	32.271	0.275	0.011
50.28	0.608	4.095	28.988	0.232	0.011
53.79	0.802	4.283	26.791	0.199	0.010
60.08	1.264	4.513	22.785	0.157	0.011
64.97	1.868	4.447	19.771	0.120	0.010
70.30	2.643	4.256	16.473	0.098	0.011
75.47	3.619	3.836	13.396	0.079	0.012
80.13	4.591	3.351	10.652	0.068	0.014
84.85	5.686	2.729	7.959	0.060	0.017
89.91	7.005	1.891	5.212	0.052	0.024
95.07	8.347	1.002	2.444	0.049	0.058

Table 3.4 Density data for the Cyrene/H_2O TM case as a function of "the initial mol fraction of Cyrene in H_2O". [293.15 K]

Initial wt% of Cyrene in H_2O	Initial mol fraction of Cyrene in H_2O	*density run 1 TM-H_2O*	*density run 2 TM-H_2O*	*density run 3 TM-H_2O*	average density TM-H_2O
0.000	**0.000**	*0.99820*	*0.99820*	*0.99820*	**0.998**
1.269	**0.002**	*0.999886*	*0.999876*	*0.99862*	**0.999**
5.366	**0.008**	*1.01713*	*1.01714*	*1.01714*	**1.017**
10.124	**0.016**	*1.03446*	*1.03446*	*1.03446*	**1.034**
14.748	**0.024**	*1.05204*	*1.05204*	*1.05204*	**1.052**
20.217	**0.034**	*1.07342*	*1.07342*	*1.07342*	**1.073**
20.101	**0.034**	*1.07297*	*1.07298*	*1.07298*	**1.073**
19.923	**0.034**	*1.00213*	*1.07064*	*1.07231*	**1.048**
25.210	**0.045**	*1.09354*	*1.09354*	*1.09354*	**1.094**
29.998	**0.057**	*1.11335*	*1.11335*	*1.11335*	**1.113**
35.009	**0.070**	*1.13452*	*1.13453*	*1.13453*	**1.135**
39.574	**0.084**	*1.15399*	*1.15399*	*1.15400*	**1.154**
39.851	**0.085**	*1.15510*	*1.15512*	*1.15512*	**1.155**
39.902	**0.085**	*1.14820*	*1.15474*	*1.15538*	**1.153**
44.692	**0.102**	*1.17570*	*1.17572*	*1.17572*	**1.176**
49.941	**0.123**	*1.19739*	*1.19741*	*1.19742*	**1.197**
55.091	**0.147**	*1.21775*	*1.21776*	*1.21775*	**1.218**
59.620	**0.172**	*1.23352*	*1.23358*	*1.23360*	**1.234**
59.871	**0.173**	*1.23448*	*1.23456*	*1.23460*	**1.235**
64.939	**0.207**	*1.24864*	*1.24882*	*1.24890*	**1.249**
69.916	**0.246**	*1.25880*	*1.25898*	*1.25906*	**1.259**
74.912	**0.296**	*1.26515*	*1.26521*	*1.26525*	**1.265**

79.959	**0.359**	*1.26739*	*1.26705*	*1.26719*	**1.267**
85.047	**0.444**	*1.26694*	*1.26701*	*1.26706*	**1.267**
89.773	**0.552**	*1.26484*	*1.26483*	*1.26482*	**1.265**
94.850	**0.721**	*1.25895*	*1.25897*	*1.25906*	**1.259**
100.000	**1.000**	*1.25175*	*1.25175*	*1.25180*	**1.252**

Table 3.5 Density data for the Cyrene/D_2O TM case as a function of "the initial mol fraction of Cyrene in D_2O". [293.15 K]

Initial wt% of Cyrene in D_2O	**Initial mol fraction of Cyrene in D_2O**	***density 1 D_2O***	***density 2 D_2O***	***density 3 D_2O***	**average density D_2O**
0.000	**0.000**	*1.10551*	*1.10551*	*1.10551*	**1.106**
0.955	**0.002**	*1.10847*	*1.10848*	*1.10848*	**1.109**
5.098	**0.008**	*1.12159*	*1.12159*	*1.12159*	**1.122**
10.078	**0.017**	*1.13776*	*1.13777*	*1.13777*	**1.138**
15.127	**0.027**	*1.15459*	*1.15459*	*1.15459*	**1.155**
19.781	**0.037**	*1.17040*	*1.17040*	*1.17041*	**1.170**
24.928	**0.049**	*1.18715*	*1.18715*	*1.18715*	**1.187**
29.921	**0.063**	*1.20567*	*1.20568*	*1.20567*	**1.206**
35.070	**0.078**	*1.22364*	*1.22365*	*1.22364*	**1.224**
40.095	**0.095**	*1.24075*	*1.24078*	*1.24077*	**1.241**
45.111	**0.114**	*1.25718*	*1.25724*	*1.25720*	**1.257**
50.124	**0.136**	*1.27249*	*1.27254*	*1.27252*	**1.273**
55.038	**0.161**	*1.28536*	*1.28543*	*1.28545*	**1.285**
59.714	**0.188**	*1.29524*	*1.29510*	*1.29516*	**1.295**
65.000	**0.225**	*1.30225*	*1.30240*	*1.30234*	**1.302**
69.965	**0.267**	*1.30408*	*1.30418*	*1.30423*	**1.304**
75.022	**0.319**	*1.30305*	*1.30300*	*1.30299*	**1.303**
80.071	**0.386**	*1.29784*	*1.29781*	*1.29783*	**1.298**
84.925	**0.468**	*1.28990*	*1.28987*	*1.28973*	**1.290**
89.940	**0.583**	*1.27958*	*1.27957*	*1.27949*	**1.280**
94.958	**0.746**	*1.26644*	*1.26646*	*1.26641*	**1.266**
100	**1.000**	*1.25175*	*1.25175*	*1.25180*	**1.252**

Table 3.6 Tabulated composition of the ternary Cyrene/ geminal diol/ D_2O mixture (TM-D_2O) as a function of the initial amount of Cyrene added to D_2O (in wt%). [298 K]

wt% Cyrene in D_2O	mol geminal diol/ mol Cyrene	mol D_2O/ mol Cyrene
94.01	0.11	0.34
90.43	0.26	0.59
84.89	0.37	1.19
80.37	0.74	1.98
74.86	0.99	3.29
64.98	2.29	9.05
60.05	3.35	15.17
54.75	4.69	25.39
49.90	6.24	40.26
45.02	8.07	62.80
40.01	10.10	96.39
34.97	12.27	145.60
30.21	14.40	213.24
25.20	16.58	317.35
20.41	18.80	475.26
15.16	20.82	760.11
9.98	23.61	1396.11
5.43	25.29	2903.83
5.03	25.00	3118.55

Figure 1A SAXS data for pure Cyrene and Cyrene/D_2O mixtures as a function of composition.

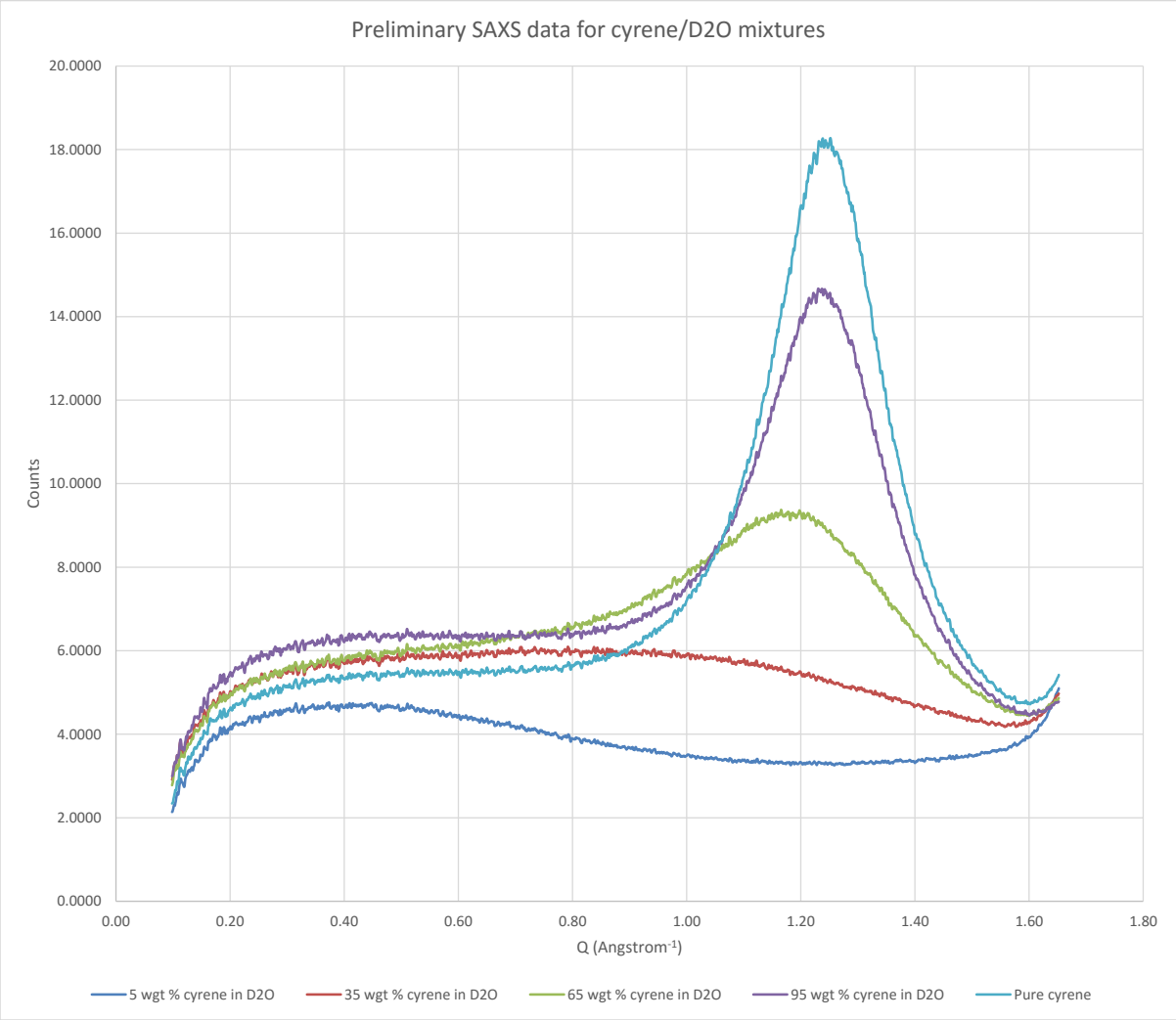

Figure 2A ESI(+) mass-spectrum of 80 wt% Cyrene in H_2O.

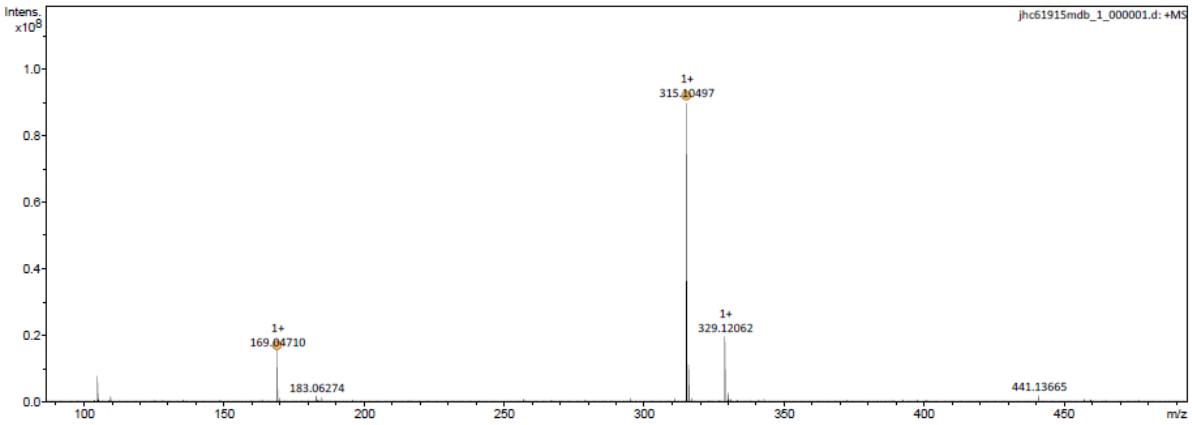

Meas. m/z	#	Ion Formula	m/z	err [ppm]	err [mDa]	mSigma	Mean err [ppm]
169.047103	1	C6H10NaO4	169.047129	0.2	0.0	7.1	0.1
315.104972	1	C12H20NaO8	315.105038	0.2	0.1	4.4	0.3

- $C_6H_{10}NaO_4$ is the sodium adduct of monomeric geminal diol
- $C_{12}H_{20}NaO_8$ is the sodium adduct of dimeric geminal diol

Table 3.7 Viscosity data for the Cyrene/H_2O TM case as a function of "the initial mol fraction of Cyrene in H_2O".

wt% of Cyrene in H_2O	Initial mol fraction of Cyrene in H_2O	viscosity average (cP)
25.011	**0.045**	**2.04**
30.016	**0.057**	**3.05**
34.638	**0.069**	**3.17**
39.974	**0.086**	**4.09**
44.401	**0.101**	**5.17**
49.945	**0.123**	**7.14**
54.545	**0.144**	**9.16**
59.434	**0.171**	**12.59**
65.210	**0.209**	**16.63**
69.903	**0.246**	**19.16**
74.984	**0.297**	**21.16**
80.205	**0.363**	**20.86**
85.212	**0.448**	**19.26**
89.917	**0.556**	**16.42**
94.746	**0.717**	**12.83**
100.000	**1.000**	**11.03**

Table 3.8 Solubilities of aspirin, salicylic acid, ferulic acid and phthalic acid as a function of the wt% of Cyrene in H_2O. [293 K]

wt% Cyrene	Salicylic acid (mol L^{-1})	wt% Cyrene	Aspirin (mol L^{-1})	wt% Cyrene	Ferulic acid (mol L^{-1})	wt% Cyrene	Phthalic acid (mol L^{-1})	wt% Cyrene	Ibuprofen (mol L^{-1})
100.00	0.684	100.00	0.293	100.00	0.195	100.00	0.049	100.00	0.684
97.20	1.088	97.50	0.720	**94.86**	**0.504**	95.09	0.211	**97.14**	**0.988**
94.64	1.355	**95.00**	**0.926**	**90.08**	**0.575**	89.98	0.353	**95.00**	**1.019**
92.42	1.494	**89.67**	**0.923**	**84.97**	**0.585**	**84.86**	**0.406**	**92.47**	**1.023**
89.35	**1.654**	84.63	0.881	80.18	0.523	**79.77**	**0.437**	89.91	0.933
84.81	1.551	80.09	0.774	75.25	0.442	**75.27**	**0.419**	85.12	0.719
79.49	1.489	74.63	0.663	70.00	0.386	70.20	0.413	80.21	0.540
77.49	1.220	70.15	0.482	64.94	0.256	65.37	0.352	75.19	0.302
74.76	1.0649	64.83	0.337	59.83	0.164	60.16	0.269	70.06	0.136
70.43	0.983	60.11	0.256	54.95	0.109	55.01	0.223	64.86	0.047
64.91	0.521	54.84	0.153	49.91	0.058	50.04	0.156		
59.88	0.316	49.93	0.109						
50.20	0.118	45.16	0.073						
39.83	0.047	29.89	0.039						
19.91	0.011	25.15	0.029						
10.28	0.007	9.92	0.019						
		8.90	0.017						

Table 3.9 Experimental solubilities of mandelic acid and caffeine as a function of the wt% of Cyrene in H_2O. [293 K]

wt% Cyrene	Mandelic acid (mol L^{-1})	wt% Cyrene	Caffeine (mol L^{-1})
100.00	1.661	100.00	0.097
95.00	3.397	94.93	0.250
89.91	4.374	89.89	0.420
85.03	**4.92**	85.01	0.462
80.07	**4.709**	**80.17**	**0.517**
75.07	**4.729**	**75.12**	**0.509**
70.11	4.667	**70.03**	**0.520**
64.93	4.592	65.07	0.475
63.27	5.631	59.99	0.475
62.36	5.48	54.91	0.414
59.73	5.738	50.37	0.385
54.96	5.347	45.15	0.259
49.74	4.868	39.99	0.214
45.12	4.720	30.18	0.172
40.09	4.182	19.83	0.148
34.85	3.551	9.91	0.115
30.18	3.673		
27.46	2.887		
25.74	2.698		
22.58	2.444		
19.92	2.578		
17.60	1.92		

14.67	1.635		
10.64	1.498		
5.19	1.210		

Table 3.10 Data on relative solubility increases vis-à-vis water and ranges of maximum solubility.

Compound	MW	Solubility in water g L^{-1} / (mol L^{-1})	Maximum attainable solubility in TM-H_2O (mol L^{-1})	wt% Cyrene in H_2O range at which maximum dissolution is observed	Maximal increase in solubility vis-à-vis solubility in water (factor)	Log Kow
Aspirin (acetyl-salicylic acid)	180.159	**4.6 (0.025)**	0.923-0.926	89.67-95.00	**36.3**	1.19
Salicylic acid	138.122	**2.24 (0.016)**	1.654	89.35	**102**	2.26
Phthalic acid	166.132	**6.25 (0.038)**	0.406-0.436	75.27-84.86	**11.6**	0.73
Ferulic acid	194.186	**5.97 (0.031)**	0.504-0.585	84.97-94.86	**19.0**	1.51
Ibuprofen	206.285	**0.021 (1.018 E-04)**	0.988-1.023	92.47-97.14	**10047**	3.97
Caffeine	194.194	**21.6 (0.111)**	0.509-0.52	70.03-80.17	**4.67**	-0.07
Mandelic acid	152.149	**181 (1.189)**	**5.738**	**59.73**	**4.13**	0.62

Table 3.11 Data on relative solubility increases vis-à-vis Cyrene and ranges of maximum solubility.

Compound	MW	Solubility in Cyrene ($mol\ L^{-1}$)	Maximum attainable solubility in TM-H_2O ($mol\ L^{-1}$)	wt% Cyrene in H_2O range at which maximum dissolution is observed	Maximal increase in solubility vis-à-vis solubility in Cyrene (factor)	Log Kow
Aspirin (acetyl-salicylic acid)	180.159	**0.293**	0.923- 0.926	89.67-95.00	**3.15**	1.19
Salicylic acid	138.122	**0.684**	1.654	89.35	**2.41**	2.26
Phthalic acid	166.132	**0.049**	0.406-0.437	75.27-84.86	**8.94**	0.73
Ferulic acid	194.186	**0.195**	0.504-0.585	84.97-94.86	**2.99**	1.51
Ibuprofen	206.285	**0.684**	0.988-1.023	92.47-97.14	**1.49**	3.97
Caffeine	194.194	**0.097**	0.509-0.52	70.03-80.17	**5.33**	-0.07
Mandelic acid	152.149	**1.661**	**4.708-4.919**	**75.07-85.03**	**2.96**	0.62

Figure 3A ^{1}H NMR spectra showing the evolution of a 65 wt% Cyrene in H_2O mixture when increasing the temperature from 298K to 358K.

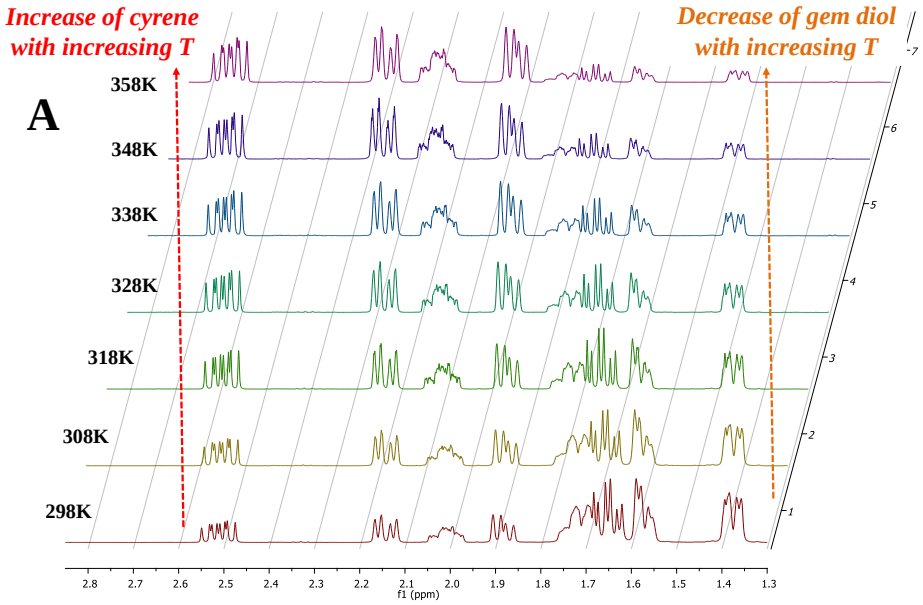

Figure 4A ^{1}H NMR spectra showing the evolution of a 65 wt% Cyrene in H_2O mixture when decreasing the temperature from 298K to 258K.